Electronic Supplementary Material (ESI) for Physical Chemistry Chemical Physics.

Electronic Supplementary Information

Influence of a Single Ether Bond on Assembly, Orientation, and Miscibility of Phosphocholine Lipids at the Air-Water Interface

Matthias Hoffmann[1,2], Simon Drescher[3,4], Christian Schwieger[2]*, Dariush Hinderberger[1,2]*

[1] Institute of Chemistry, Martin Luther University (MLU) Halle-Wittenberg, Von-Danckelmann-Platz 4, 06120 Halle (Saale), Germany

[2] Interdisciplinary Research Center HALOmem, MLU Halle-Wittenberg, Charles Tanford Protein Center, Kurt-Mothes-Str. 3a, 06120 Halle (Saale), Germany

[3] Institute of Pharmacy, MLU Halle-Wittenberg, Wolfgang-Langenbeck-Str. 4, 06120 Halle (Saale), Germany

[4] Phospholipid Research Center, Im Neuenheimer Feld 515, 69120 Heidelberg, Germany

Synthesis and purification of PHPC

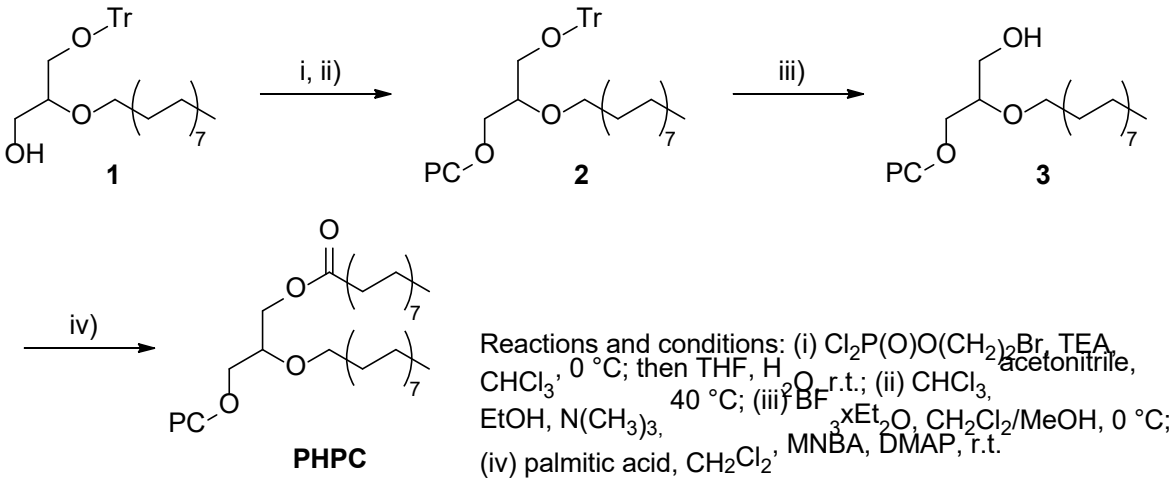

Scheme S1. Synthesis of PHPC. (Tr – trityl; PC – phosphocholine)

Synthetic procedures

The synthesis of *rac*-1-palmitoyl-2-*O*-hexadecyl-*sn*-glycero-3-phosphocholine (PHPC) is based on the methodology described previously (S. Lindner *et al.* Azide-modified Membrane Lipids: Synthesis, Properties, and Reactivity. *Langmuir* **2017**, *33*, 4960) using a total synthetic approach and *rac*-1-*O*-trityl-2-*O*-hexadecyl-*sn*-glycerol (**1**) (also termed 2-(hexadecyl)-3-(triphenylmethoxy)-1-propanol) (Brachwitz, H.; Langen, P.; Otto, A.; Schildt, J., Halogenlipide. III. Alkyl-glyceryl-ether-Analoga, *J. Prakt. Chem.* **1979**, 321, 775-786) as starting compound.

*Introduction of the PC headgroup: Synthesis of rac-1-O-trityl-2-O-hexadecyl-sn-glycero-3-phosphocholine (**2**)*

We used a method described by Eibl & Nicksch (Eibl, H.; Nicksch, A., 1,3-Propanedeol phosphatides. *Ger. Offen.* DE 2345057 A1 19750327, 27.03.1975) using 2-bromo-ethylphosphoric acid dichloride as the phosphorylating reagent, which was introduced by Hirt & Berchtold (Hirt, G.; Berchtold, R., Synthesis of phosphatides. A new synthesis of lecithin. *Pharm. Acta Helv.* **1958**, *33*, 349).

2-Bromoethylphosphoric acid dichloride (8 equiv.) was poured into dry chloroform under cooling with ice/water. A mixture of dry triethylamine (TEA) (14 equiv.) and dry chloroform was added slowly with stirring, which was continued for 30 min at 0 °C. The alcohol **1** (1 equiv.) was added as solid substance in one portion. The suspension was heated until the solid was dissolved, then cooled to room temperature. Stirring was continued for a further 24-48 h at room temperature. After thin layer chromatography (TLC) showed complete conversion of **1**, crushed ice was added to the solution and the mixture was stirred for a further 2 h. The organic layer was separated, and the aqueous phase was diluted with a cold saturated brine and then extracted several times with chloroform. The combined organic phases were concentrated under reduced pressure and the oily residue was dissolved in THF/H_2O (9/1). After 1.5 h the

solvent was evaporated, and the oily residue was transferred into a mixture of chloroform (3 parts), acetonitrile (3 parts) and an alcoholic solution of trimethylamine (1 part, 4.2 M). The mixture was kept in a closed tube at 40 °C for 48-72 h. After TLC showed formation of the product, the mixture was concentrated by evaporation of the solvent and the residue was purified by chromatography on silica gel by using the gradient technique and chloroform/methanol/water as eluent. Compound **2** was obtained in 65 % yield. $C_{43}H_{66}NO_6P$; ESI-MS: *m*/*z* (positive mode): 747.01 $[M + Na]^+$, 1109.05 $[3M + 2H]^{2+}$, 1470.98 $[2M + Na]^+$. ^{1}H NMR (400 MHz, $CDCl_3$, 27 °C): δ 0.88 (t, ^3J = 6.8 Hz, 3 H, CH_3), 1.23-1.31 (m, 26 H, C***H***$_2$), 1.49-1.56 (m, 2 H, OCH_2C***H***$_2CH_2$), 3.17-3.20 (m, 11 H, N(C***H***$_3)_3$ and OC***H***$_2$), 3.47-3.64 (m, 5 H, OCH_2C***H***$_2$N, OC***H***$_2$, OC***H***), 3.86-3.95 (m, 2 H, OC***H***$_2$), 4.09-4.16 (m, 2 H, OC***H***$_2CH_2$N), 7.17-7.44 (m, 15 H, 3× C_6***H***$_5$) ppm. ^{13}C NMR (100 MHz, $CDCl_3$, 27 °C): δ 14.09 (***C***H_3), 22.66 (***C***H_2CH_3), 26.18, 29.33-30.27 (***C***H_2), 31.90 (***C***$H_2CH_2CH_3$), 54.26 (N(***C***$H_3)_3$), 59.05 (NCH_2***C***H_2O), 63.92 (O***C***H_2), 65.27 (d, $^2J_{C,P}$ = 4.9 Hz, PO***C***H_2CH), 66.28 (N***C***H_2CH_2O), 70.66 (O***C***H_2), 78.58 (d, $^3J_{C,P}$ = 8.3 Hz, $POCH_2$***C***H), 86.47 (***C***$(C_6H_5)_3$), 126.92 (C4, C_6H_5), 127.73 (C3 and C5, C_6H_5), 128.77 (C2 and C6, C_6H_5), 144.04 (C1, C_6H_5) ppm.

*De-tritylation: Synthesis of rac-1-hydroxy-2-O-hexadecyl-sn-glycero-3-phospho-choline (**3**)*

For the cleavage of the trityl blocking group, BF_3×Et_2O in MeOH was used in accordance with the procedure described by Hermetter and Paltauf (Hermetter, A.; Paltauf, F., A new method for the detritylation of 1,2-diradyl-3-O-tritylglycerols. *Chem. Phys. Lipids* **1981**, *29*, 191).

Compound **2** (1 equiv.) was dissolved in dry CH_2Cl_2 (30 mL) and cooled to 0 °C. A solution of BF_3×Et_2O (1.2 equiv.) in dry MeOH (1 mL) was added slowly and the mixture was stirred for 1 h at 0 °C. Afterwards, the mixture was diluted with $CHCl_3$ (15 mL) and washed with ice-cold water (3× 20 mL). The combined organic layers were dried over Na_2SO_4 and evaporated. The crude products were purified by chromatography using $CHCl_3$/Et_2O as the solvent and the gradient technique. Compound **3** was obtained in 90 % yield. $C_{24}H_{52}NO_6P$; ESI-MS: *m*/*z* (positive mode): 482.59 $[M + H]^+$, 504.54 $[M + Na]^+$, 985.92 $[2M + Na]^+$.

*Introduction of the fatty acid: Synthesis of rac-1-palmitoyl-2-O-hexadecyl-sn-glycero-3-phosphocholine (**PHPC**)*

For the subsequent re-acylation reaction, one can use the method described by Steglich (Neises, B.; Steglich, W., Einfaches Verfahren zur Veresterung von Carbonsäuren. *Angew. Chem.* **1978**, *90*, 556) using a 1.5-fold excess of the fatty acid, 1.65 equiv. of dicyclohexylcarbodiimide (DCC), and 10 mol % of 4-(dimethylamino)pyridine (DMAP). However, we have used a different activation reagent with which we have recently had good success (S. Lindner *et al.* Azide-modified Membrane Lipids: Synthesis, Properties, and Reactivity. *Langmuir* **2017**, *33*, 4960). We used 2-methyl-6-nitrobenzoic anhydride (MNBA, 5 equiv.) following the method described by Yasuda *et al.* (T. Yasuda *et al.* Detailed Comparison of Deuterium Quadrupole Profiles between Sphingomyelin and Phosphatidylcholine Bilayers. *Biophys. J.* **2014**, *106*, 631).

To a solution of compound **3** (1 equiv.) and palmitic acid (1.5 equiv.) in CH_2Cl_2 were added MNBA (1.5 equiv.) and DMAP (3 equiv.). After the reaction mixture was stirred for 24 h at r.t., the reaction was quenched by adding MeOH and the solvent was removed under vacuum to give the crude PHPC, which was purified by column chromatography using $CHCl_3$/MeOH/H_2O as the eluent and the gradient technique. PHPC was finally freeze dried. $C_{40}H_{82}NO_7P$; ESI-MS: *m*/*z* (positive mode): 742.59 [M + Na]$^+$.

Unfortunately, we have to mention that this reaction process produced a by-product that was difficult to remove from the desired PHPC. This by-product is a coupling product of compound **3** and MNBA (see chemical structure below), which could be confirmed by MS investigations. Nevertheless, by multiple chromatography with a slowly increasing gradient it was possible to get pure PHPC.

rac-1-(2-Methyl-6-nitrobenzoyl)-2-*O*-hexadecyl-*sn*-glycero-3-phosphocholine

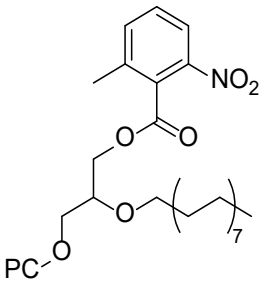

by-product

$C_{32}H_{57}N_2O_9P$; ESI-MS: *m*/*z* (positive mode): 667.33 [M + Na]$^+$.

Analytical data

rac-1-*O*-Trityl-2-*O*-hexadecyl-*sn*-glycero-3-phosphocholine (**2**) – ESI-MS

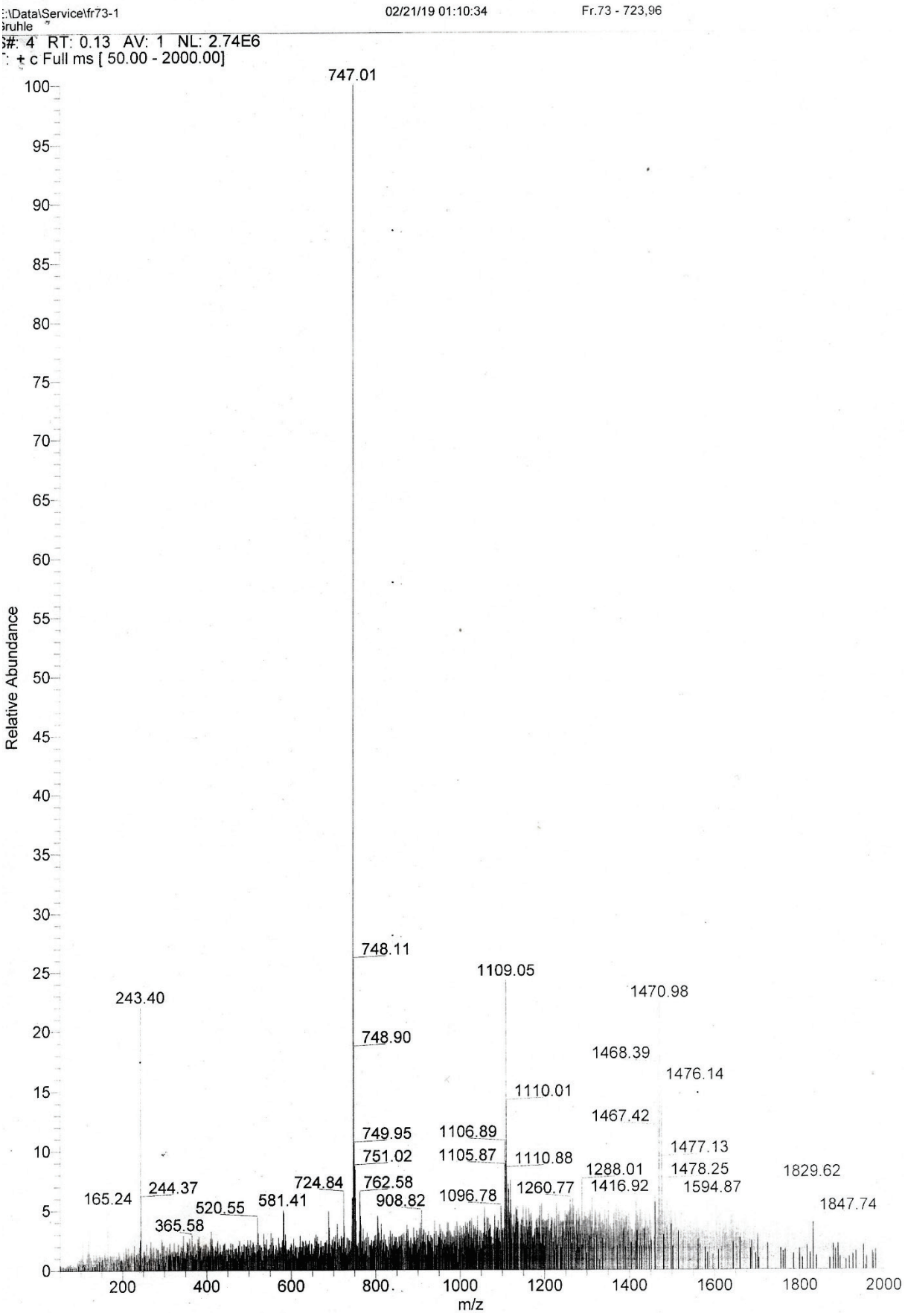

rac-1-*O*-Trityl-2-*O*-hexadecyl-*sn*-glycero-3-phosphocholine (**2**) – ^{1}H-NMR

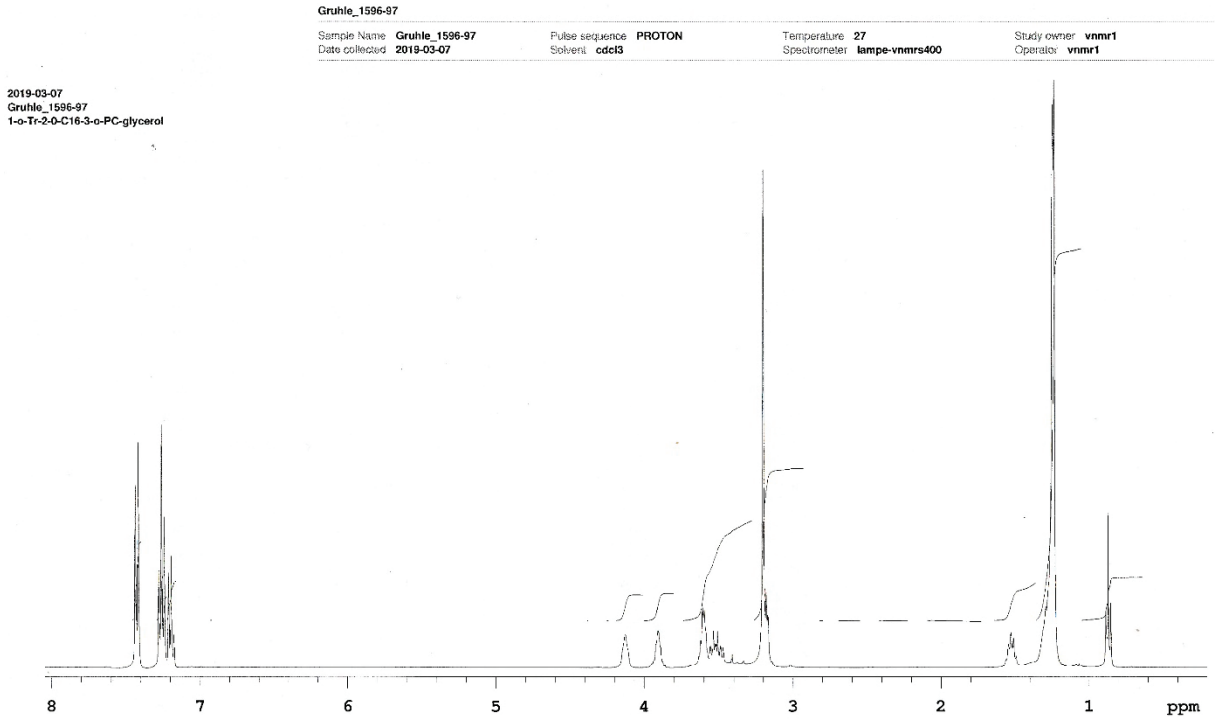

rac-1-*O*-Trityl-2-*O*-hexadecyl-*sn*-glycero-3-phosphocholine (**2**) – ^{13}C-NMR

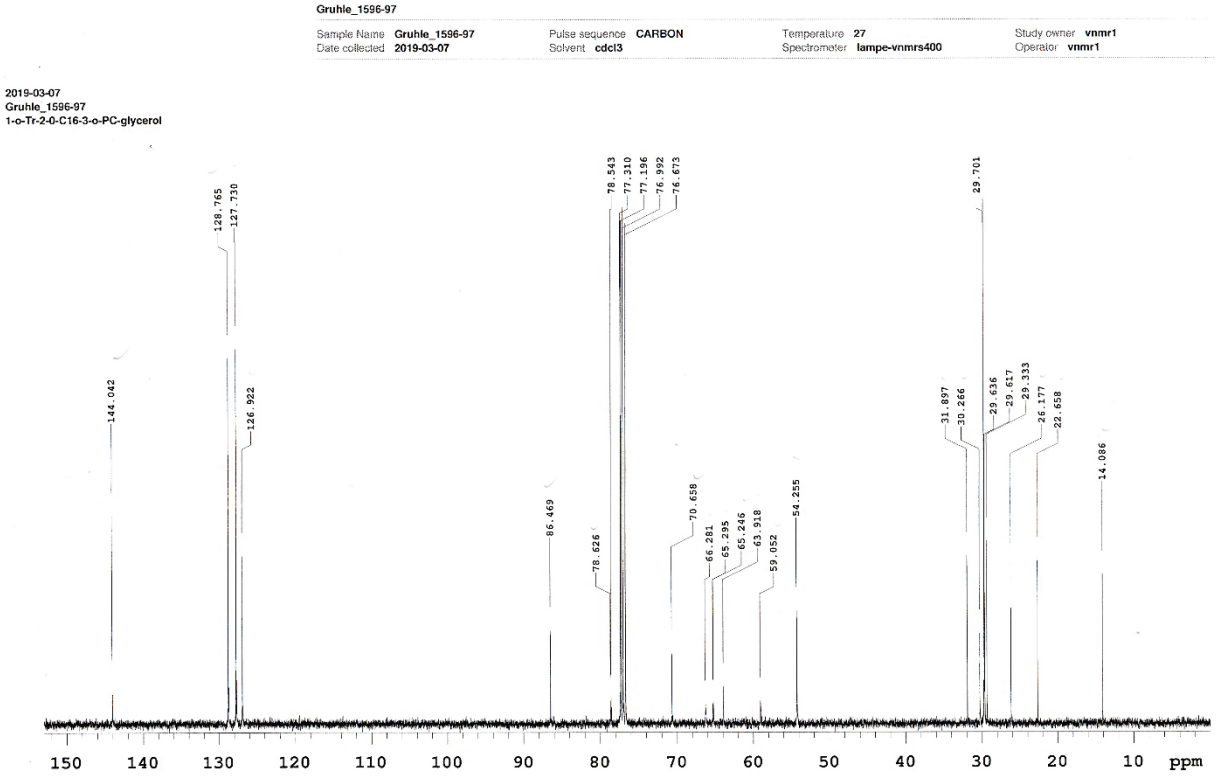

rac-1-Hydroxy-2-*O*-hexadecyl-*sn*-glycero-3-phosphocholine (**3**) – ESI-MS

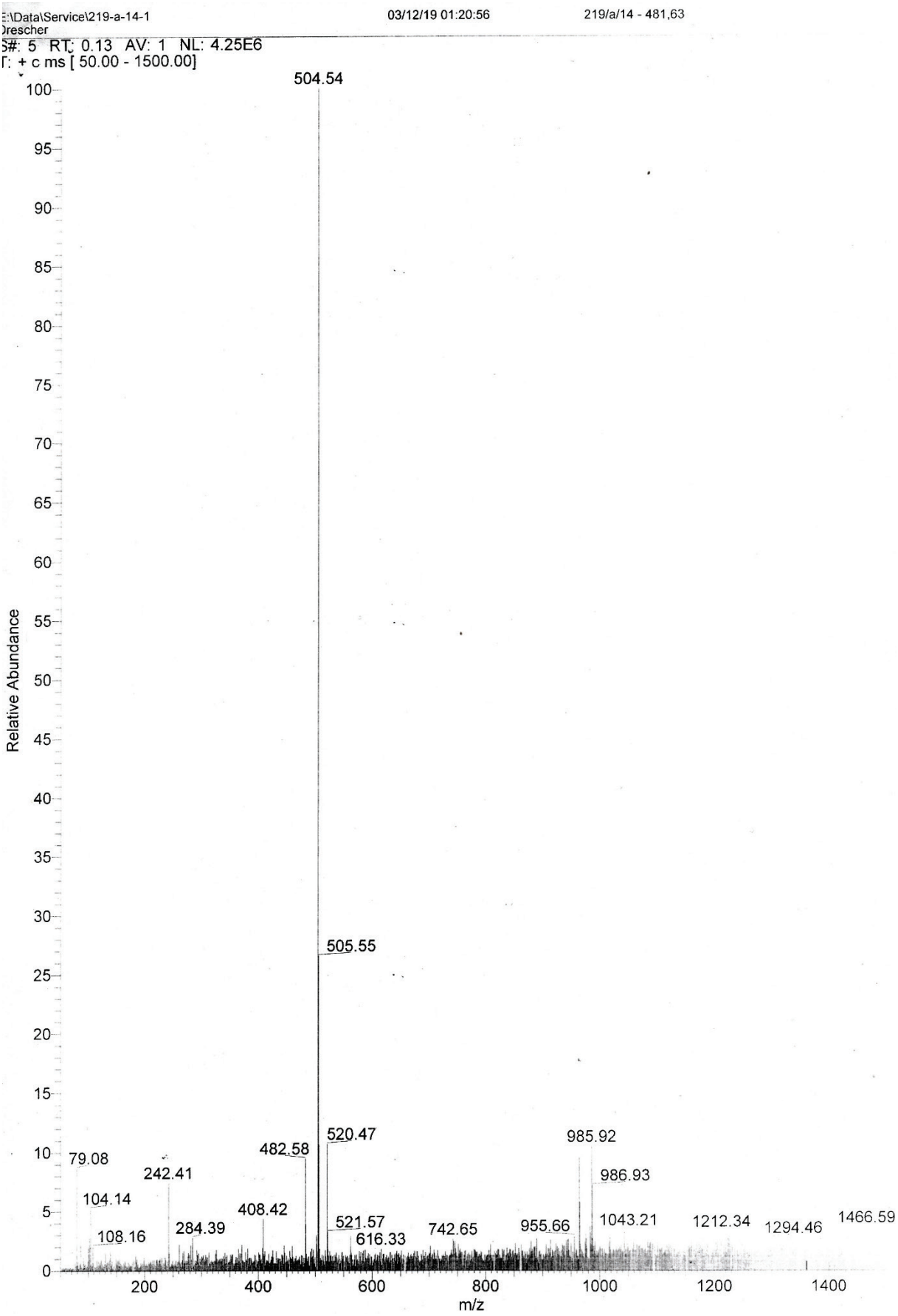

rac-1-Palmitoyl-2-*O*-hexadecyl-*sn*-glycero-3-phosphocholine (**PHPC**) – ESI-MS

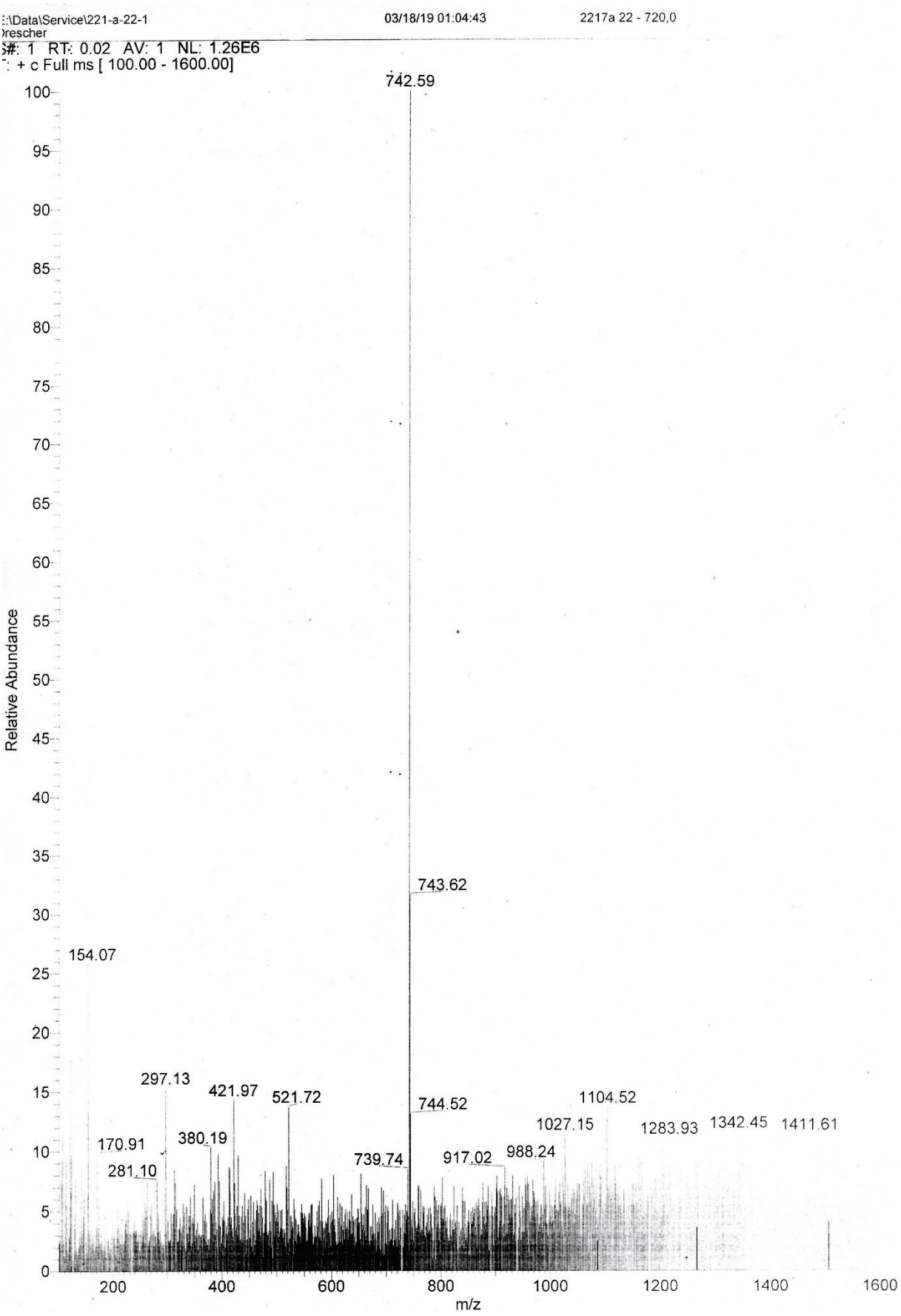

rac-1-(2-Methyl-6-nitrobenzoyl)-2-*O*-hexadecyl-*sn*-glycero-3-phosphocholine

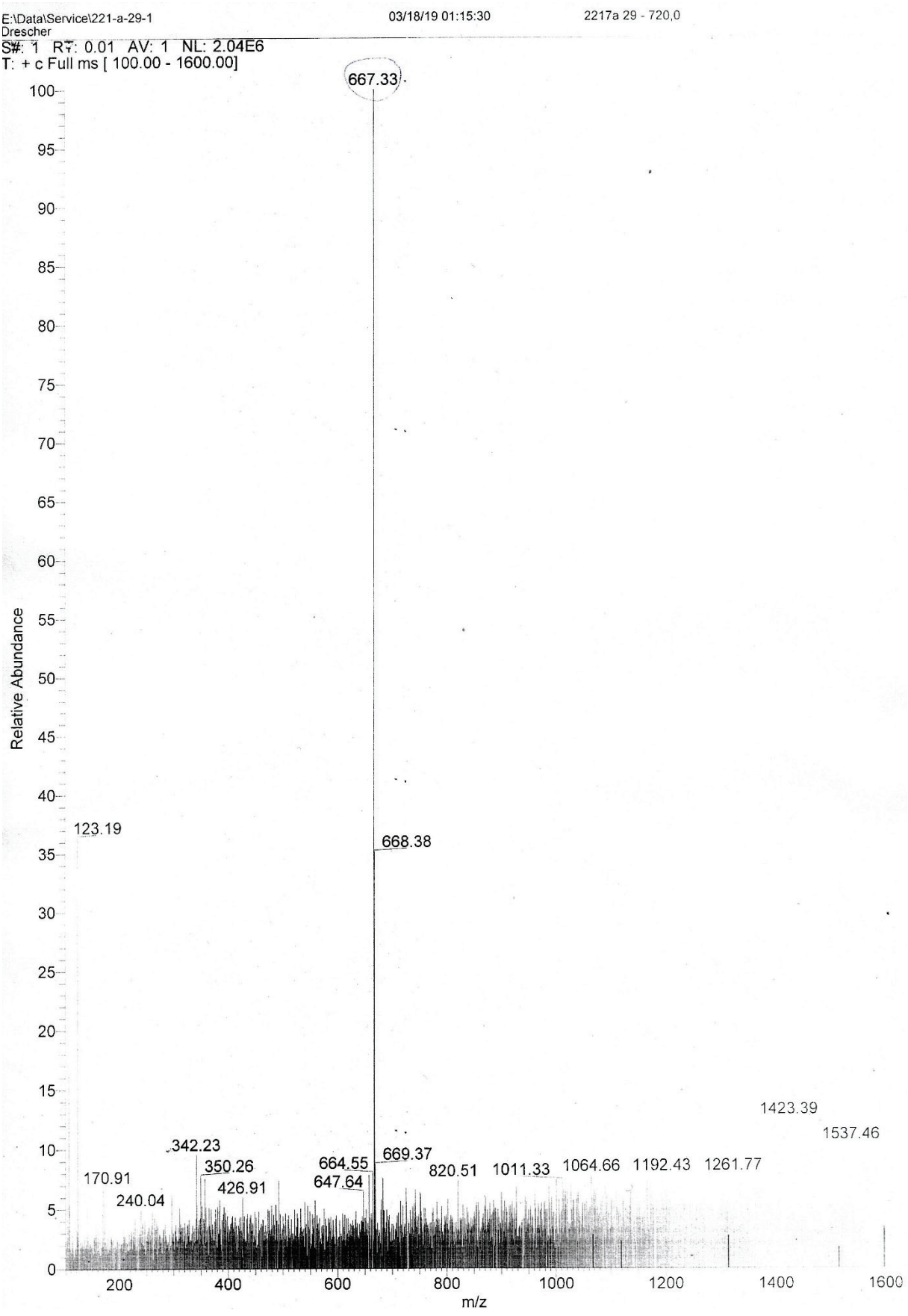

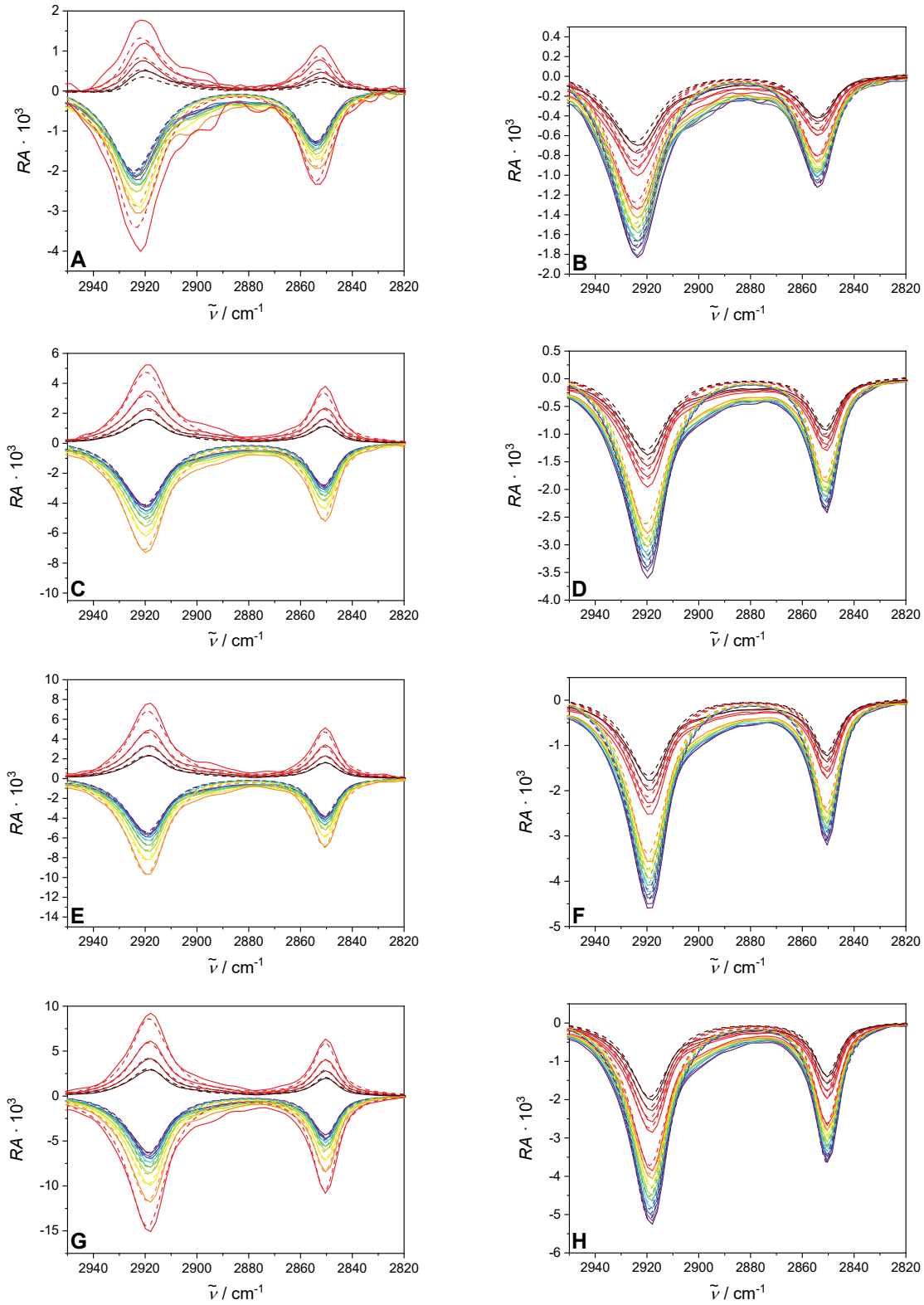

Figure S1. Angle dependent IRRA spectra of PHPC (**A/C/E/G**, p-polarized; **B/D/F/H**, s-polarized) of CH_2 stretching vibrations from top to bottom at 3 mN m^{-1} (**A/B**) in the LE phase and at 10 (**C/D**), 20 (**E/F**), and 30 mN m^{-1} (**G/H**) in the LC phase (solid lines, experimental spectra; dashed lines, calculated spectra).

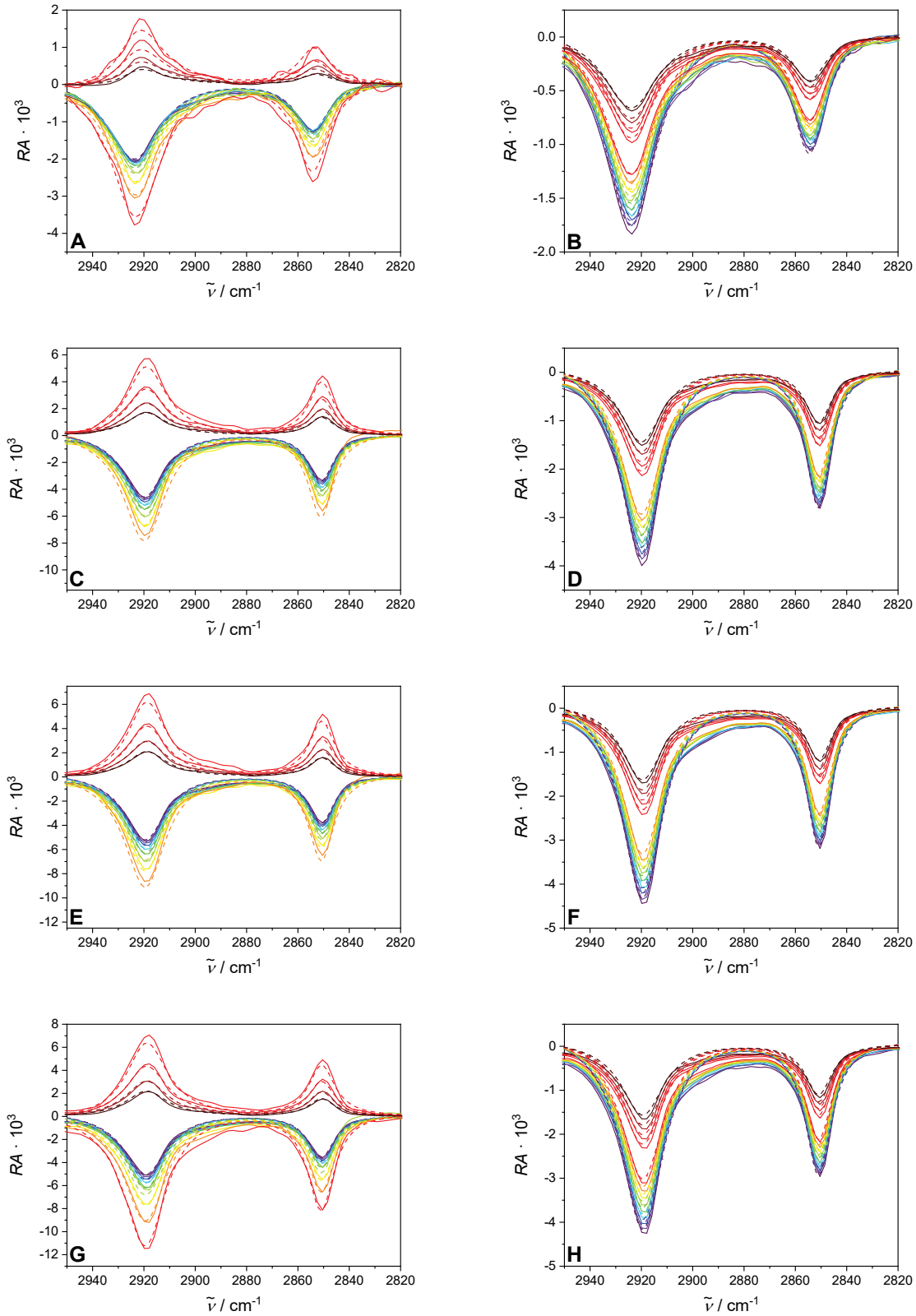

Figure S2. Angle dependent IRRA spectra of DPPC (**A/C/E/G**, p-polarized; **B/D/F/H**, s-polarized) of CH_2 stretching vibrations from top to bottom at 3 mN m^{-1} (**A/B**) in the LE phase and at 10 (**C/D**), 20 (**E/F**), and 30 mN m^{-1} (**G/H**) in the LC phase (solid lines, experimental spectra; dashed lines, calculated spectra).

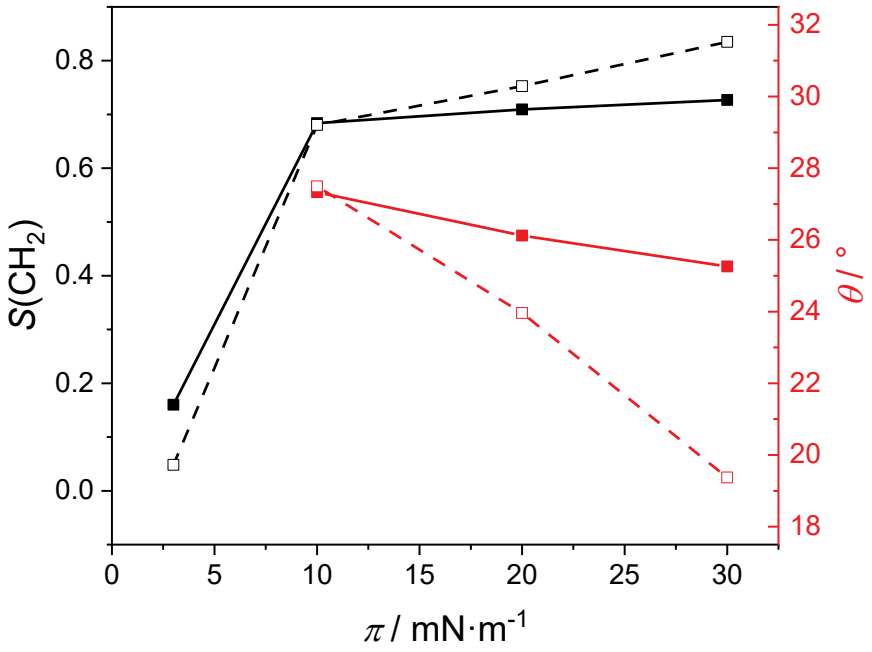

Figure S3. Pressure dependent chain order parameter (black) and tilt angle (red) of DPPC (solid lines and full squares) and PHPC (dashed lines and open squares) monolayers at 20 °C.

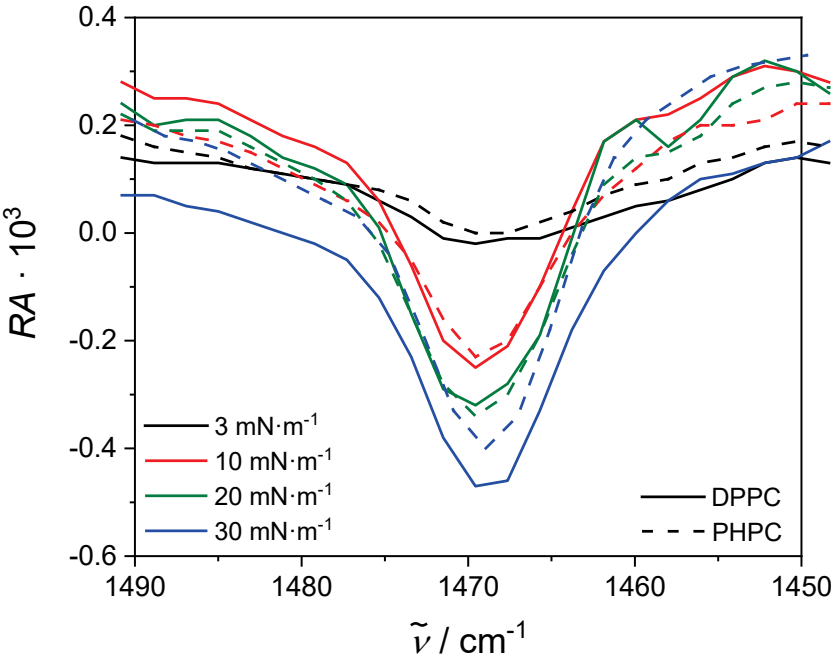

Figure S4. CH_2 scissoring band of pure PHPC (dashed lines) and DPPC (solid lines) monolayers at 20 °C at different surface pressures.

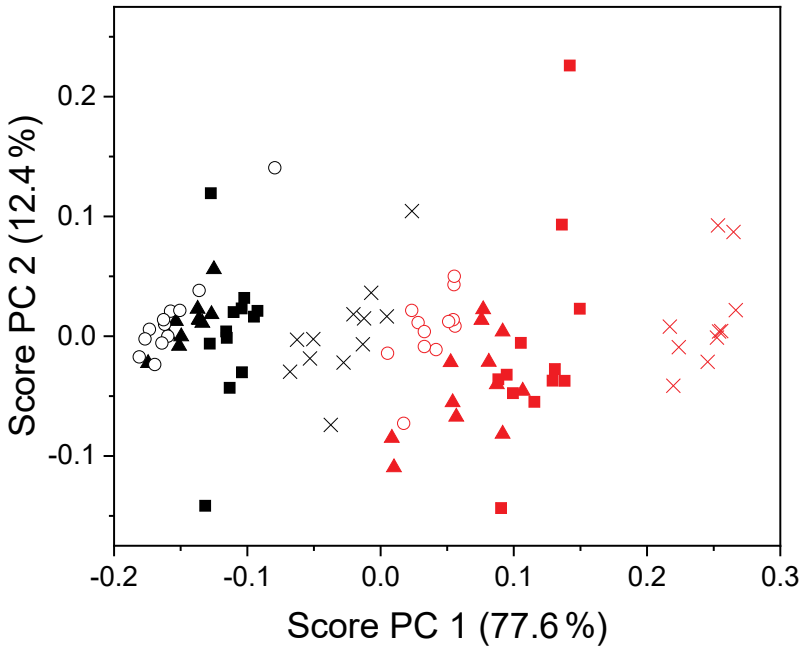

Figure S5. PCA results of the ν(C=O) band of pure PHPC and DPPC monolayers at different surface pressures showing the scores of PC 1 *versus* PC 2. The IRRAS data used in this PCA were measured in the LE phase of both lipids (3 mN m^{-1}, cross symbols) and in the LC phase (10 mN m^{-1}, squares; 20 mN m^{-1}, triangles; and 30 mN m^{-1}, open circles) of DPPC (black symbols) and PHPC (red symbols), respectively.

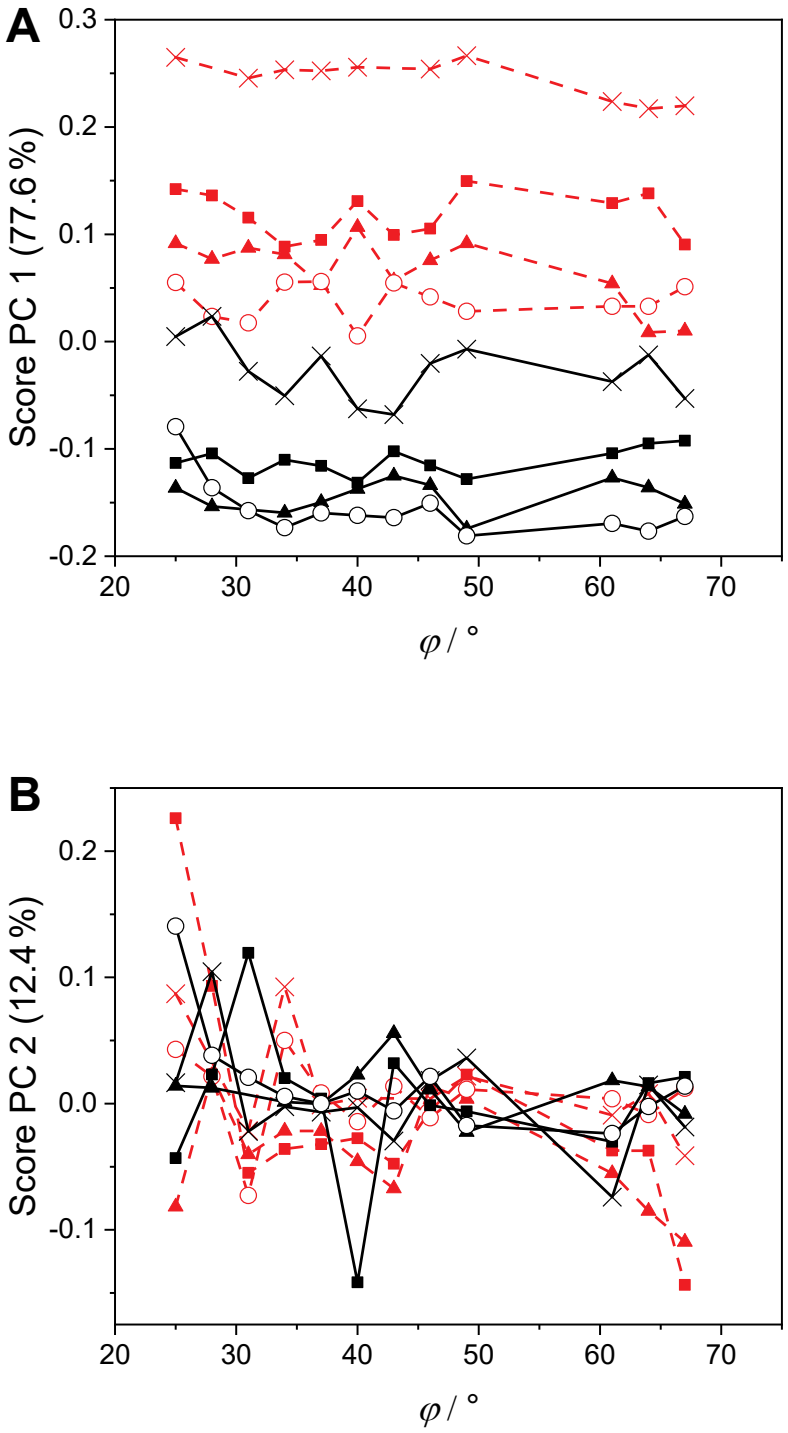

Figure S6. PCA Results of the ν(C=O) band of pure PHPC (red symbols) and DPPC (black symbols) monolayers at different surface pressures. **A**: scores of PC 1 plotted versus φ, **B**: scores of PC 2 versus φ. The IRRAS data used in this PCA was measured in the LE phase of both lipids (3 mN m^{-1}, cross symbols) and in the LC phase (10 mN m^{-1}, squares; 20 mN m^{-1}, triangles; 30 mN m^{-1}, open circles) of DPPC and PHPC, respectively.

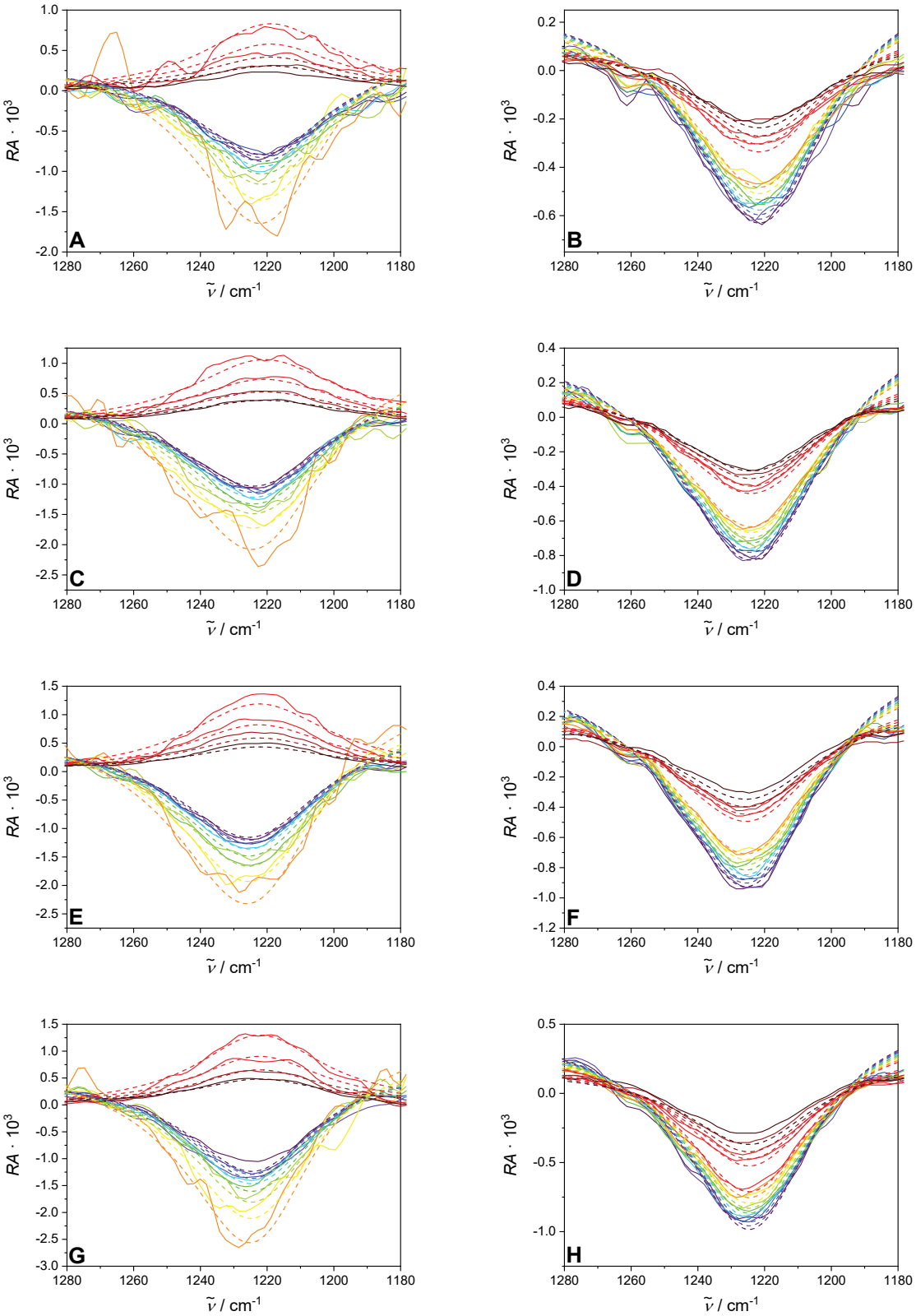

Figure S7. Angle dependent IRRA spectra of PHPC (**A/C/E/G**, p-polarized; **B/D/F/H**, s-polarized) in the $\nu_{as}(PO_2^-)$ region including CH_2 wagging band progressions from top to bottom at 3 mN m^{-1} (**A/B**) in the LE phase and at 10 (**C/D**), 20 (**E/F**), and 30 mN m^{-1} (**G/H**) in the LC phase (solid lines, experimental spectra; dashed lines, calculated spectra). **G/H** are additionally shown in **Figure 4C** and **D**.

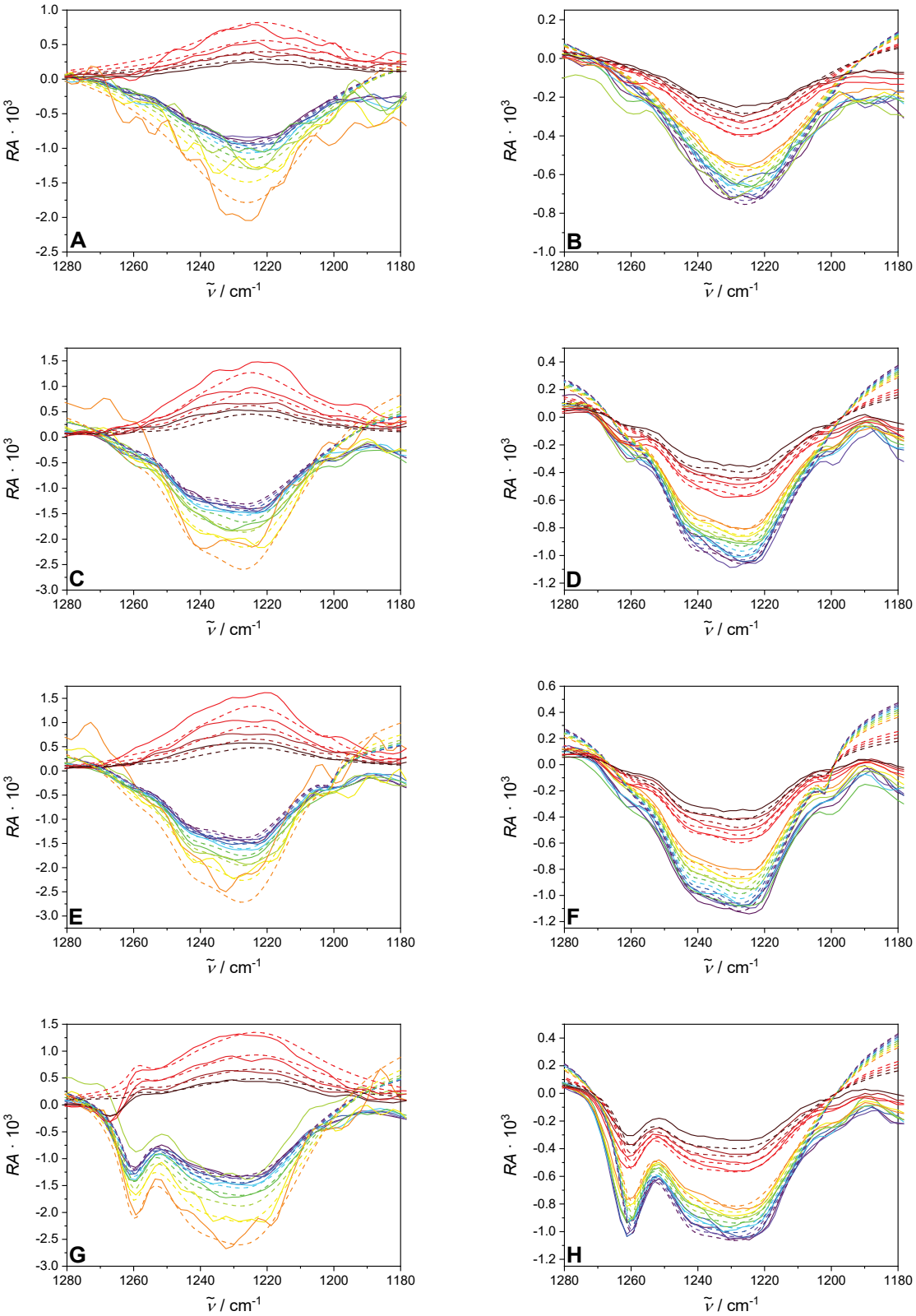

Figure S8. Angle dependent IRRA spectra of DPPC (**A/C/E/G**, p-polarized; **B/D/F/H**, s-polarized) in the $\nu_{as}(PO_2^-)$ region including CH_2 wagging band progressions from top to bottom at 3 mN m^{-1} (**A/B**) in the LE phase and at 10 (**C/D**), 20 (**E/F**), and 30 mN m^{-1} (**G/H**) in the LC phase (solid lines, experimental spectra; dashed lines, calculated spectra). **G/H** are additionally shown in **Figure 4A** and **B**.

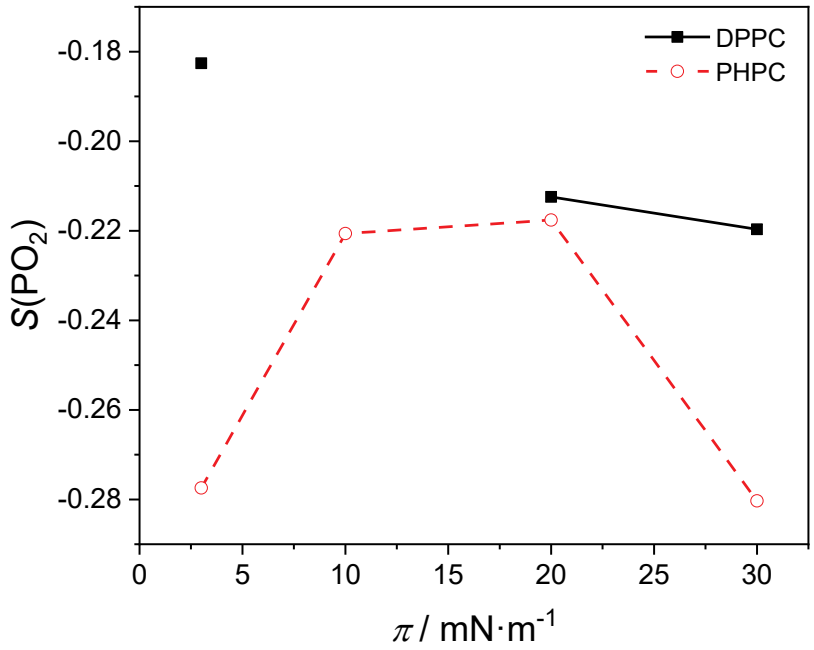

Figure S9. Pressure dependent order parameter of the phosphate group in DPPC (solid lines and full squares) and PHPC (dashed lines and open circles) monolayers at 20 °C and α = 0°. At 10 mN m^{-1} the $\nu_{as}(PO_2^-)$ of DPPC could not be fitted with α = 0°.

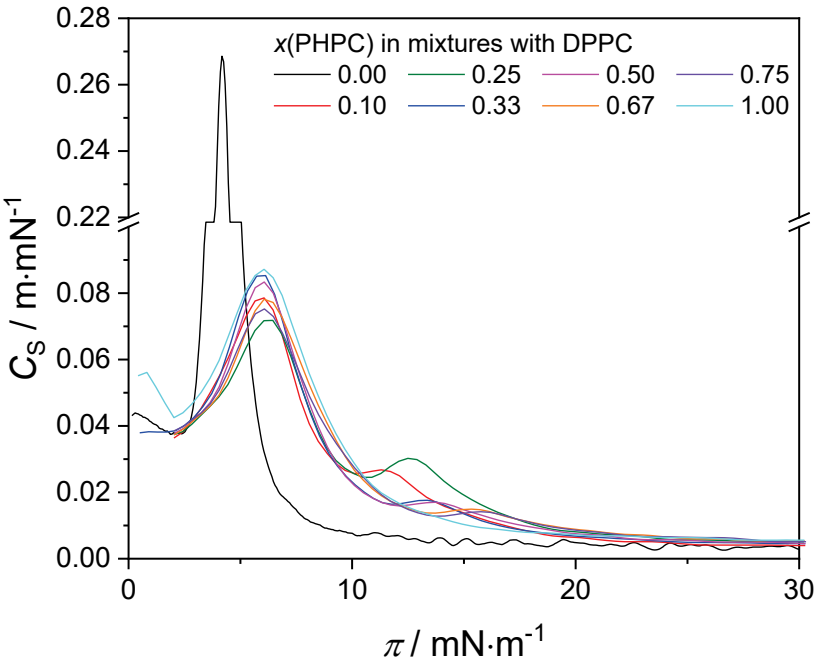

Figure S10. Compressibilities of mixed PHPC/DPPC monolayers of various compositions, derived from the isotherms shown in **Figure 5** (main article). The maxima of C_S are used to determine plateau surface pressures for the mixed monolayers as shown also in **Figure 5**.

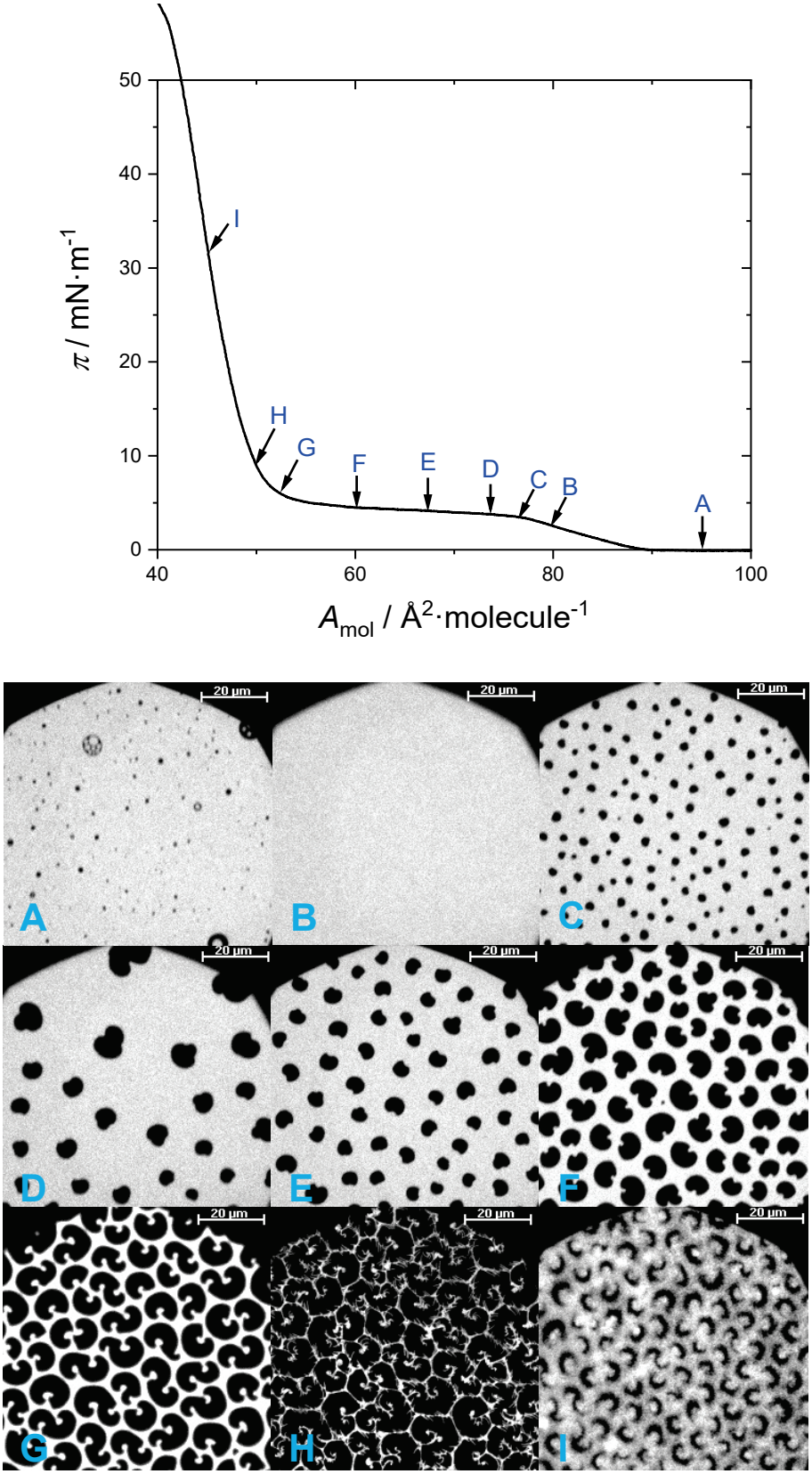

Figure S11. Epifluorescence microscopy of a DPPC monolayer. Shown are the π–A_{mol} isotherm as well as several micrographs taken during compression of the monolayer as indicated.

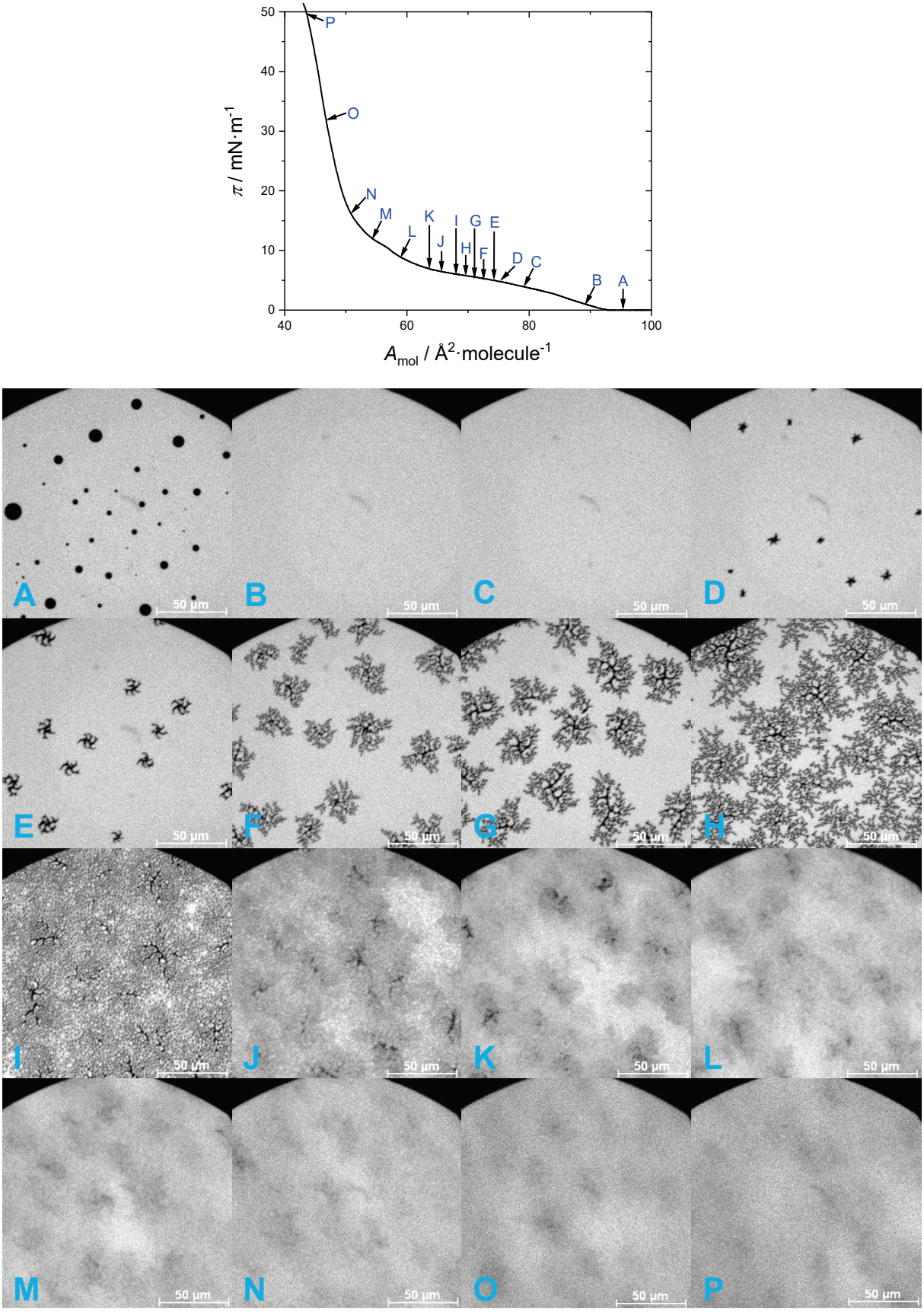

Figure S12. Epifluorescence microscopy of a mixed monolayer of DPPC/PHPC 9:1 (x(PHPC) = 0.10). Shown are the π–A_{mol} isotherm as well as several micrographs taken during compression of the monolayer as indicated.

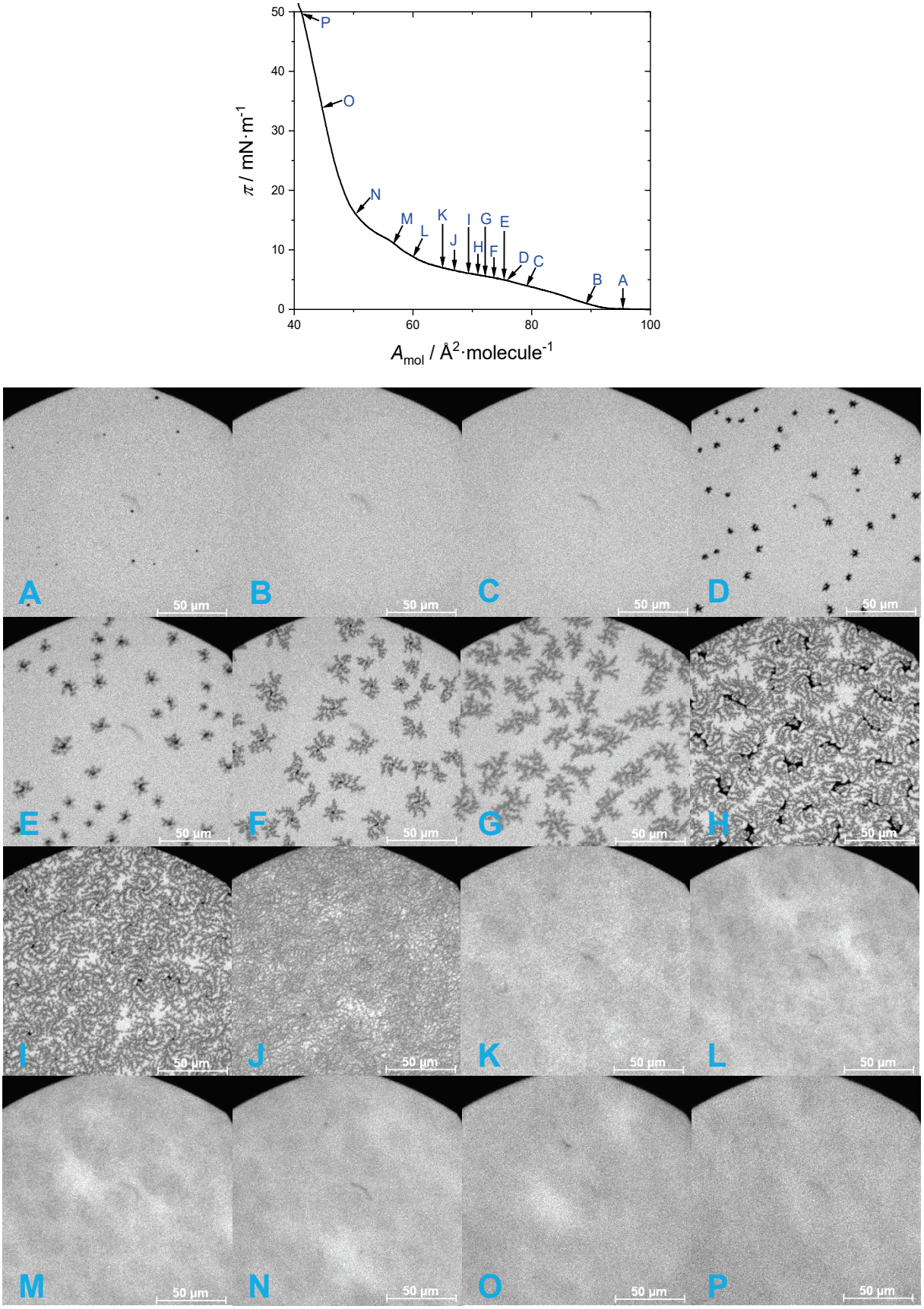

Figure S13. Epifluorescence microscopy of a mixed monolayer of DPPC/PHPC 3:1 (x(PHPC) = 0.25). Shown are the π–A_{mol} isotherm as well as several micrographs taken during compression of the monolayer as indicated.

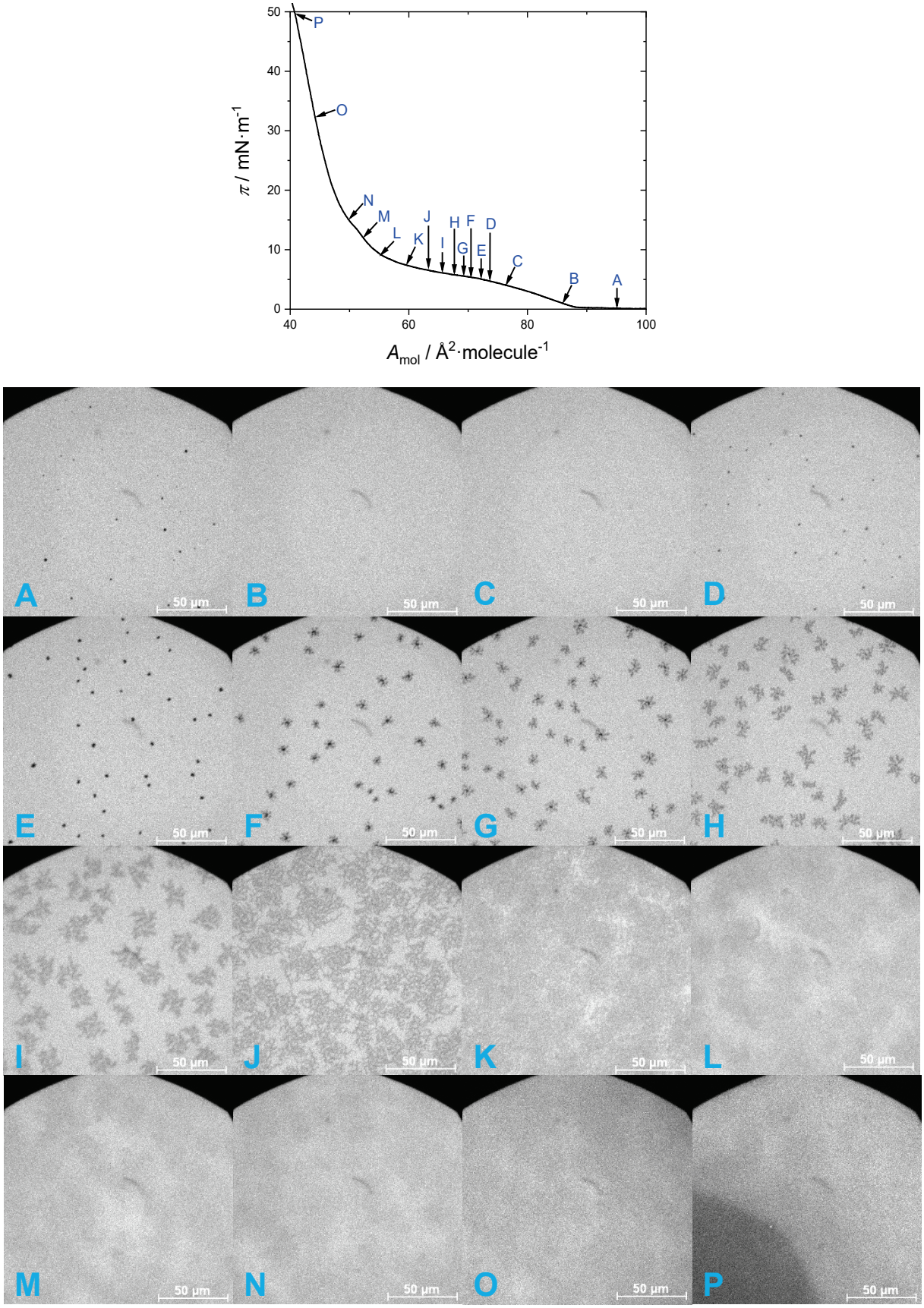

Figure S14. Epifluorescence microscopy of a mixed monolayer of DPPC/PHPC 1:1 (x(PHPC) = 0.50). Shown are the π–A_{mol} isotherm as well as several micrographs taken during compression of the monolayer as indicated.

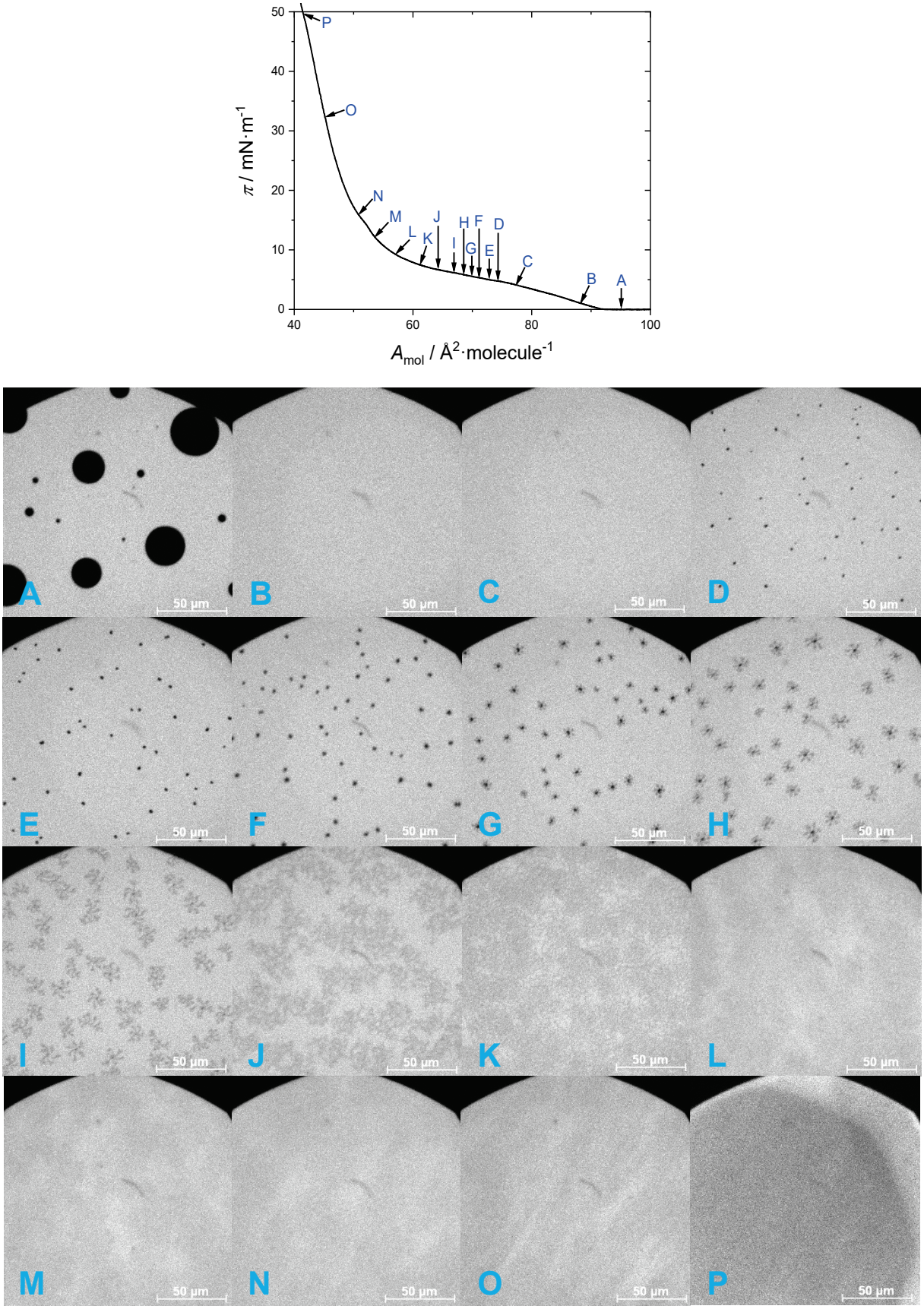

Figure S15. Epifluorescence microscopy of a mixed monolayer of DPPC/PHPC 1:3 (x(PHPC) = 0.75). Shown are the π–A_{mol} isotherm as well as several micrographs taken during compression of the monolayer as indicated.

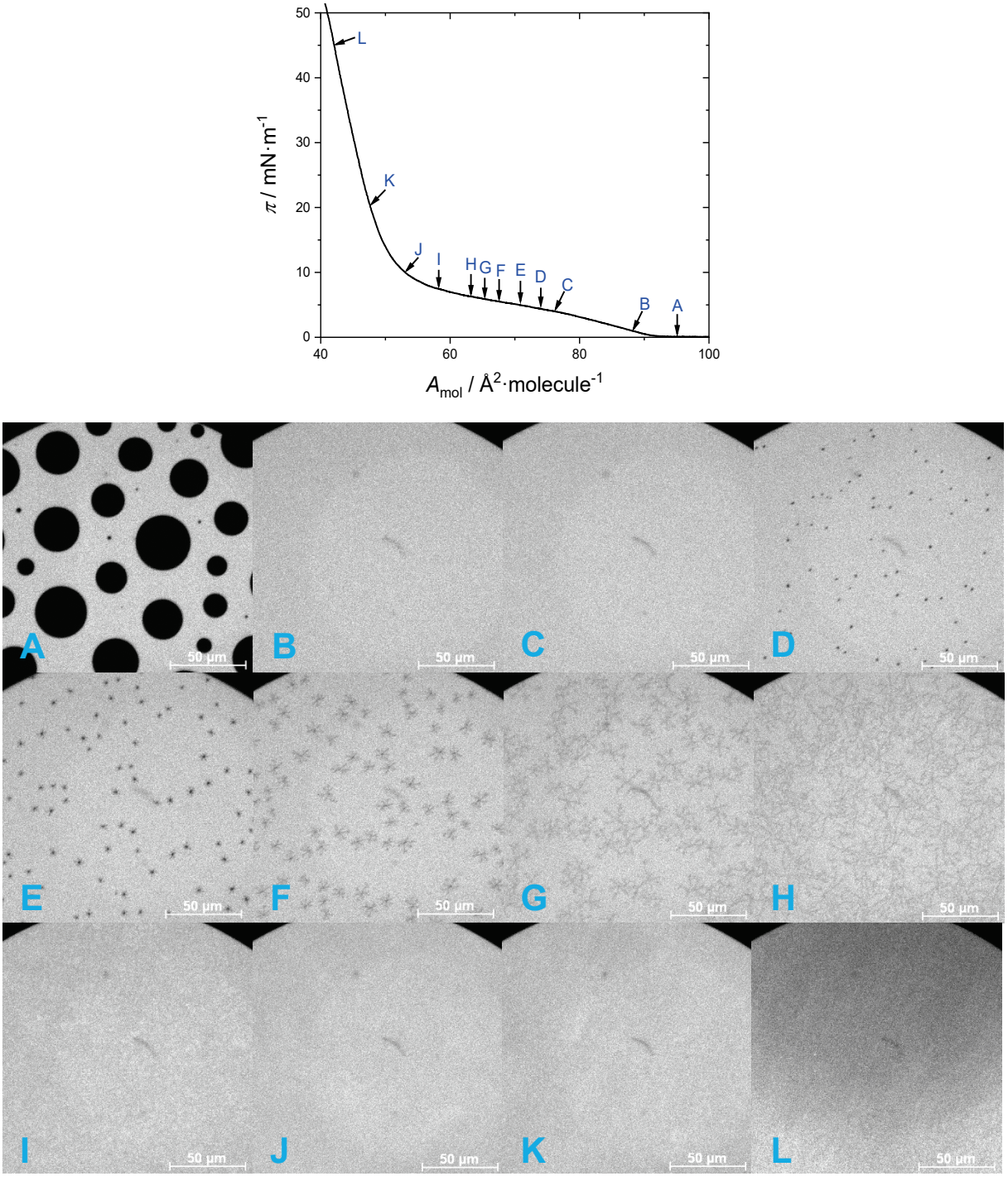

Figure S16. Epifluorescence microscopy of a PHPC monolayer. Shown are the π–A_{mol} isotherm as well as several micrographs taken during compression of the monolayer as indicated.

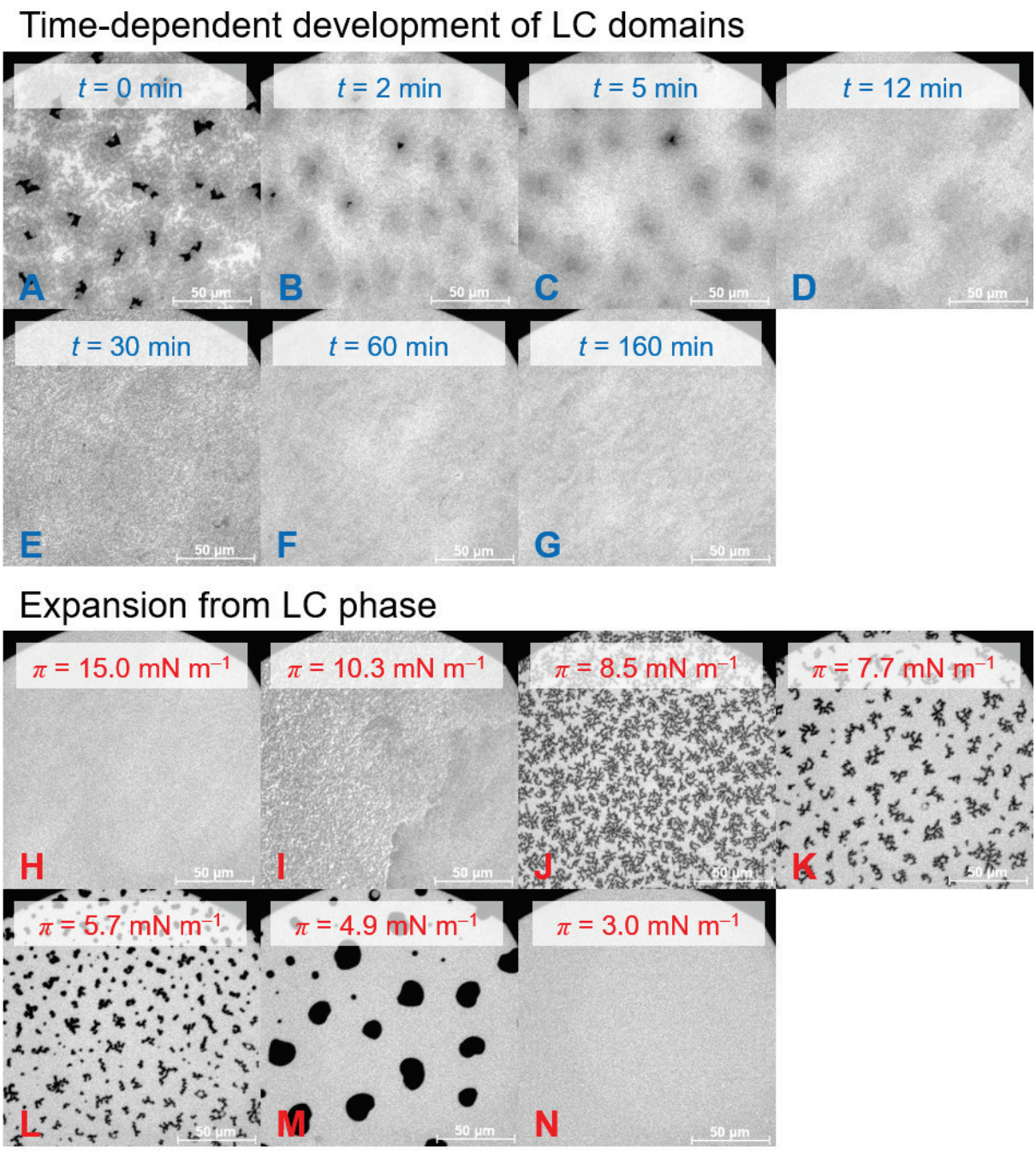

Figure S17. Epifluorescence microscopy of a mixed monolayer of DPPC/PHPC 9:1 (x(PHPC) = 0.10). Shown is the time dependent development of the LC domains (**A-G**) as well as an expansion experiment (**H-N**). For the first experiment, the isothermal compression was stopped at the end of the LE/LC transition. π was kept constant at 9.2 mN m^{-1} for the times indicated in the micrographs. For the second experiment, the monolayer was compressed to 15 mN m^{-1} and, subsequently, expanded again. The surface pressures at which images were recorded are indicated in the micrographs.

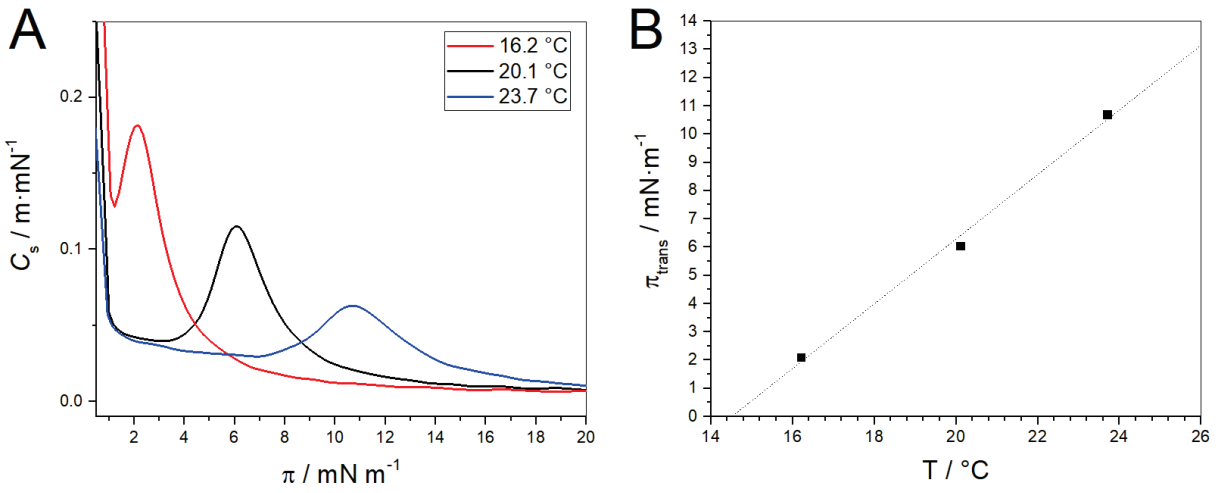

Figure S18. A: Compressibilities of a DPPC/PHPC 3:1 mixed monolayer at different temperatures derived from the corresponding isotherms (not shown). **B**: The maxima of C_S *versus* the temperature of the experiment.

Table S1. Miscibility studies of PHPC and DPPC in monolayers; ΔG_{exc} and ΔG_{mix} at different surface pressures.

x(PHPC)	3 mN m^{-1}		10 mN m^{-1}		30 mN m^{-1}	
	ΔG_{exc} / kJ mol^{-1}	ΔG_{mix} / kJ mol^{-1}	ΔG_{exc} / kJ mol^{-1}	ΔG_{mix} / kJ mol^{-1}	ΔG_{exc} / kJ mol^{-1}	ΔG_{mix} / kJ mol^{-1}
0.10	0.01	-0.78	0.30	-0.49	0.38	-0.41
	± 0.06	± 0.06	± 0.26	± 0.26	± 0.53	± 0.53
0.25	-0.02	-1.39	0.21	-1.16	0.10	-1.27
	± 0.06	± 0.06	± 0.23	± 0.23	± 0.46	± 0.46
0.33	-0.05	-1.59	0.09	-1.46	-0.02	-1.56
	± 0.05	± 0.05	± 0.13	± 0.13	± 0.34	± 0.34
0.50	-0.05	-1.74	0.07	-1.62	-0.05	-1.74
	± 0.06	± 0.06	± 0.18	± 0.18	± 0.41	± 0.41
0.67	-0.02	-1.57	0.11	-1.43	0.02	-1.52
	± 0.04	± 0.04	± 0.14	± 0.14	± 0.49	± 0.49
0.75	0.01	-1.36	0.20	-1.17	0.29	-1.08
	± 0.01	± 0.01	± 0.01	± 0.01	± 0.18	± 0.18

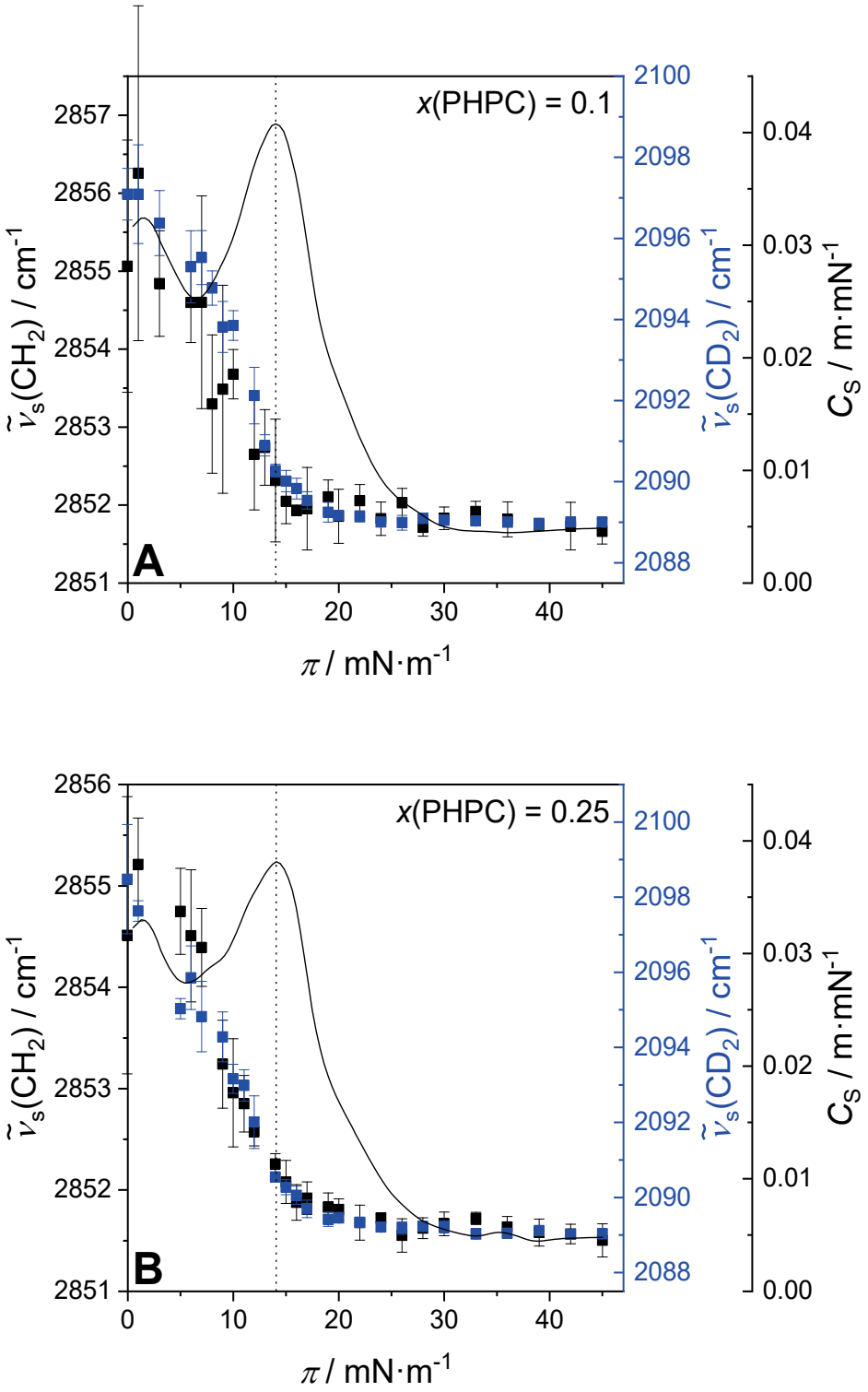

Figure S19. Frequency of the CH_2 and CD_2 symmetric stretching vibrations and monolayer compressibility during compression of mixed PHPC/DPPC-d_{62} monolayers at various lipid ratios as given in each graph, measured at 20 °C.

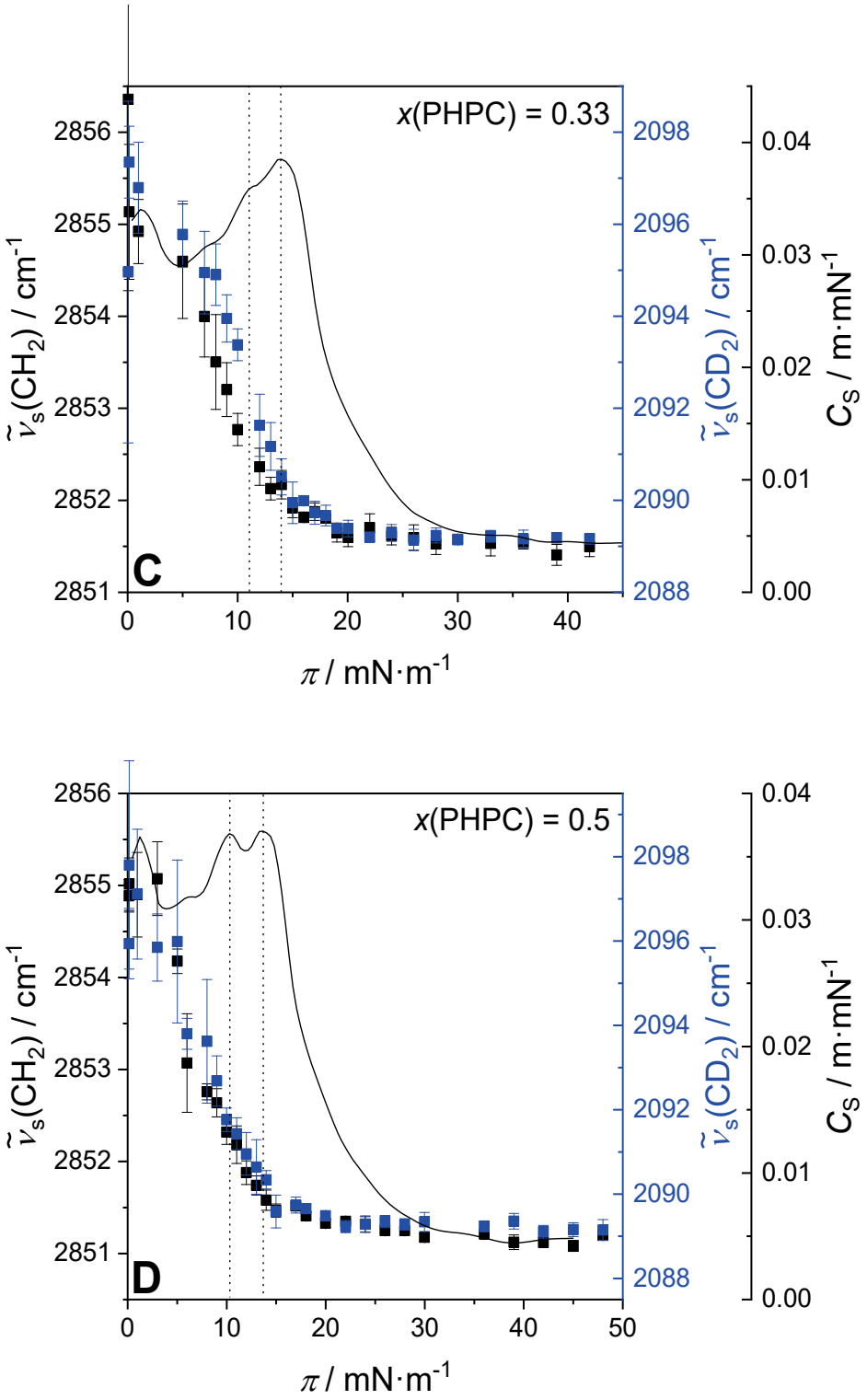

Figure S19 continued. Frequency of the CH_2 and CD_2 symmetric stretching vibrations and monolayer compressibility during compression of mixed PHPC/DPPC-d_{62} monolayers at various lipid ratios as given in each graph, measured at 20 °C.

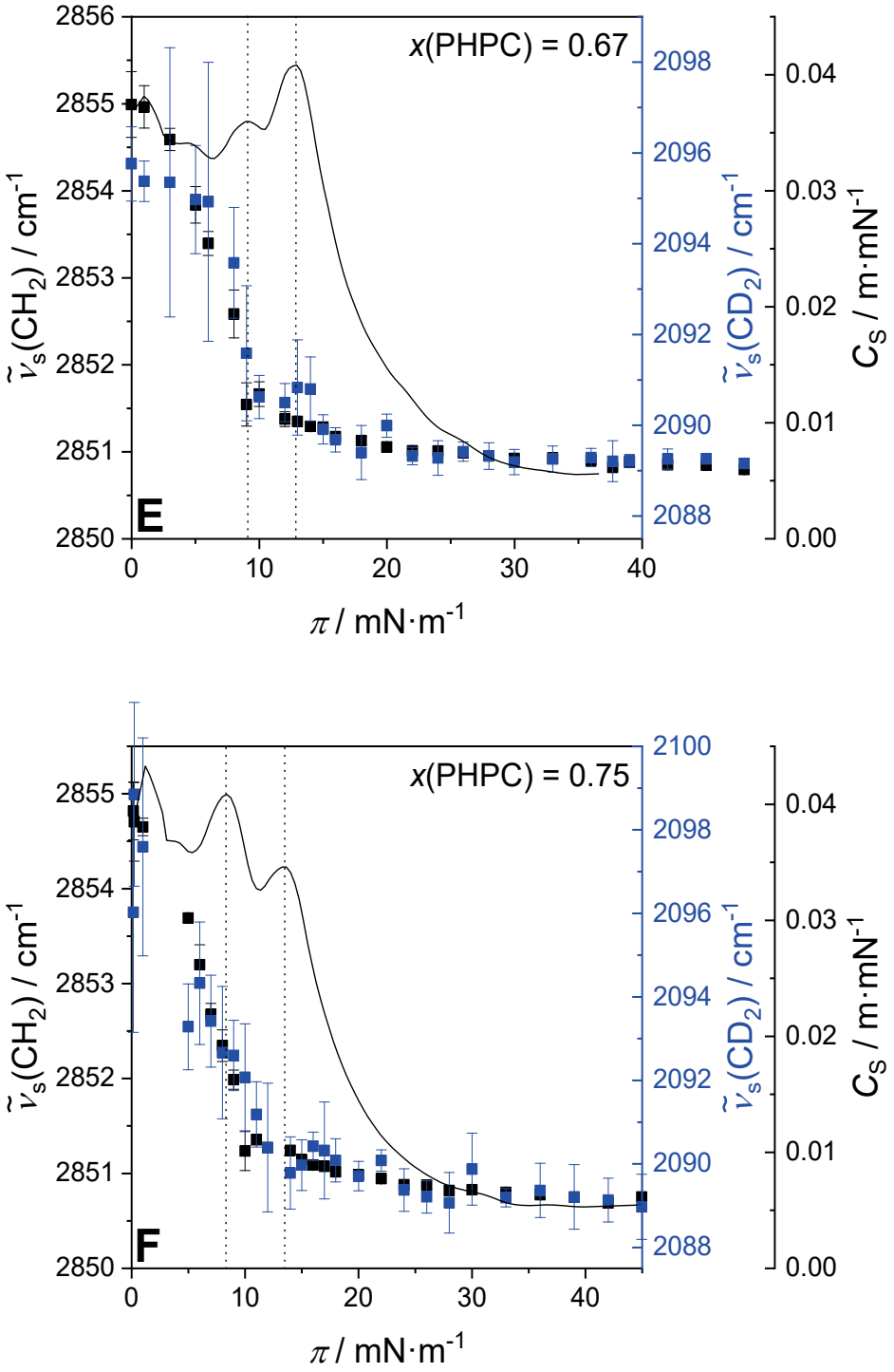

Figure S19 continued. Frequency of the CH_2 and CD_2 symmetric stretching vibrations and monolayer compressibility during compression of mixed PHPC/DPPC-d_{62} monolayers at various lipid ratios as given in each graph, measured at 20 °C.

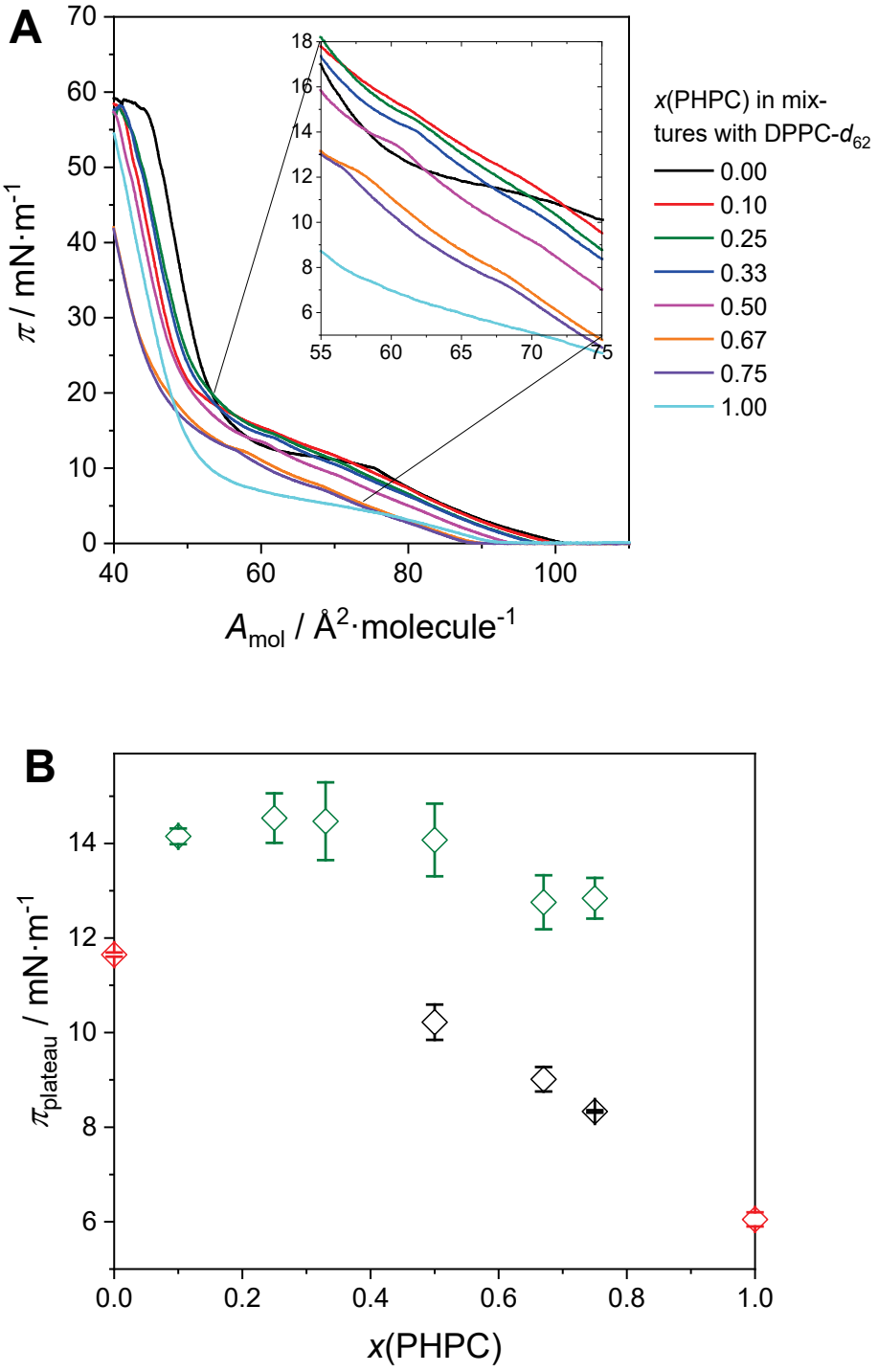

Figure S20. π–A_{mol} isotherms of DPPC-d_{62}/PHPC mixtures and derived plateau surface pressures. **A**: π–A_{mol} isotherms with π range of the upper plateau in the inset, **B**: part of the phase diagram with all observed $\pi_{plateau}$ (pure DPPC-d_{62} and PHPC are marked red). In the mixtures containing less than 50 % PHPC $\pi_{plateau}$ of the lower plateau could not be determined, but the observed C_S peak was broadened (compare **Figure S19**).

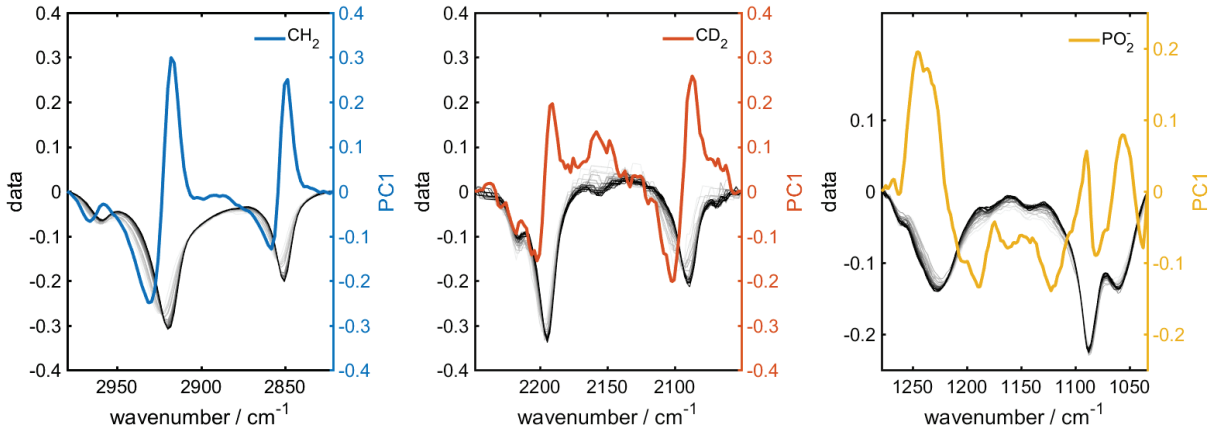

Figure S21. Loadings of PC 1 of a PCA of the CH_2 stretching vibrations (left, blue line), the CD_2 stretching vibrations (middle, orange line), and the phosphate stretching vibrations (right, yellow line) of a DPPC/PHPC 1:3 mixture at 20 °C. The grey curves in every panel show the individual IRRA spectra ranges (after vector normalization) of the mixture at various surface pressures forming the basis for the PCA.

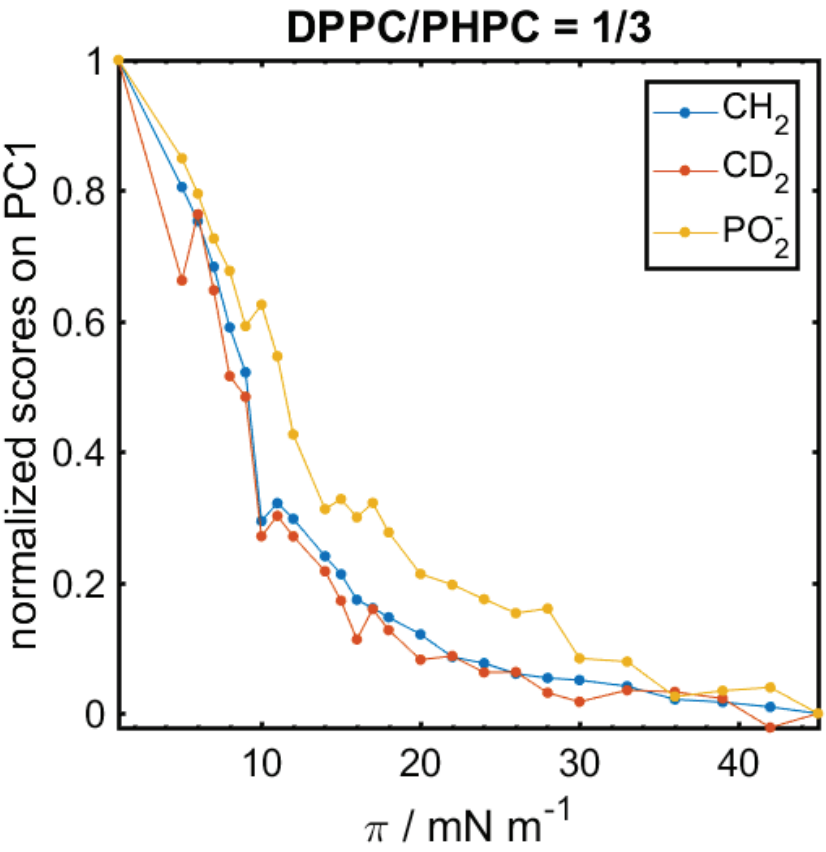

Figure S22. Normalized score on PC 1 of the CH_2 stretching vibrations (blue), the CD_2 stretching vibrations (orange), and the phosphate stretching vibrations (yellow) *versus* surface pressure π for the DPPC/PHPC 1:3 mixture. The IRRA spectra used for the PCA and the respective loadings are shown in **Figure S21**.